eNeuro

Research Article: New Research | Disorders of the Nervous System

Inhibition of IKK# Reduces Ethanol Consumption in C57BL/6J Mice

Inhibition of IKK# Reduces Ethanol Consumption

Jay M. Truitt[1], Yuri A. Blednov[1], Jillian M. Benavidez[1], Mendy Black[1], Olga Ponomareva[1], Jade Law[1], Morgan Merriman[1], Sami Horani[1], Kelly Jameson[1], Amy W. Lasek[2], R. Adron Harris[1] and R. Dayne Mayfield[1]

[1]*Waggoner Center for Alcohol and Addiction Research, The University of Texas at Austin, Austin, TX 78712, USA*

[2]*Department of Psychiatry, University of Illinois at Chicago, Chicago, IL 60612, USA.*

DOI: 10.1523/ENEURO.0256-16.2016

Received: 12 September 2016

Accepted: 12 September 2016

Published: 19 October 2016

Author Contributions: YAB, RAH, and RDM designed research; JMT, JMB, MB, OP, JL, MM, SH, and KJ performed research; JMT, OP, MM, SH, KJ, YAB, and RDM analyzed data; AWL contributed unpublished reagents/analytical tools; JMT and RDM wrote the paper.

The authors declare no competing financial interests.

Corresponding Author: R. Dayne Mayfield, Ph.D., Waggoner Center for Alcohol and Addiction Research, The University of Texas at Austin, 2500 Speedway, MBB 1.124, Austin, Texas 78712, E-mail: dayne.mayfield@austin.utexas.edu

Cite as: eNeuro 2016; 10.1523/ENEURO.0256-16.2016

Title: Inhibition of IKKβ Reduces Ethanol Consumption in C57BL/6J Mice

Abbreviated title: Inhibition of IKKβ Reduces Ethanol Consumption

Author names and affiliations: Jay M. Truitt[1], Yuri A. Blednov[1], Jillian M. Benavidez[1], Mendy Black[1], Olga Ponomareva[1], Jade Law[1], Morgan Merriman[1], Sami Horani[1], Kelly Jameson[1], Amy W. Lasek[2], R. Adron Harris[1], R. Dayne Mayfield[1]

[1]Waggoner Center for Alcohol and Addiction Research, The University of Texas at Austin, Austin, TX 78712, USA; [2]Department of Psychiatry, University of Illinois at Chicago, Chicago, IL 60612, USA.

Author Contributions: YAB, RAH, and RDM designed research; JMT, JMB, MB, OP, JL, MM, SH, and KJ performed research; JMT, OP, MM, SH, KJ, YAB, and RDM analyzed data; AWL contributed unpublished reagents/analytical tools; JMT and RDM wrote the paper.

Corresponding Author: R. Dayne Mayfield, Ph.D.

Waggoner Center for Alcohol and Addiction Research, The University of Texas at Austin, 2500 Speedway, MBB 1.124, Austin, Texas 78712

Phone: 512.232.7578

Email: dayne.mayfield@austin.utexas.edu

Number of Figures: 10

Number of Tables: 1

Number of Multimedia: 0

Number of words for Abstract: (248)

Number of words for Significance Statement: (96)

Number of words for Introduction: (622)

Number of words for Discussion: (1,253)

Acknowledgements: The authors thank Casey Wright for supplying mice and Jody Mayfield for valuable editing and writing contributions.

Conflict of Interest: The authors declare no competing financial interests.

Funding Sources: Research was supported by NIH/NIAAA grants AA012404, AA013520, AA012404, and AA0209260.

Abstract

Proinflammatory pathways in neuronal and non-neuronal cells are implicated in the acute and chronic effects of alcohol exposure in animal models and humans. Nuclear factor kappa-B (NF-κB) is a transcription factor for proinflammatory chemokines and cytokines. Inhibitory kappa-B kinase beta (IKKβ) regulates the NF-κB cascade by targeting the inhibitor of NF-κB (IκB) for degradation and represents a point of convergence for many extracellular signals. However, the role of IKKβ had not been investigated as a potential regulator of excessive alcohol drinking. Based on previous findings that overactivation of innate immune/inflammatory signaling promotes ethanol consumption, we hypothesized that inhibiting IKKβ would limit/decrease drinking by preventing activation of NF-κB. We studied the systemic effects of two pharmacological inhibitors of IKKβ, TPCA-1 and sulfasalazine, on ethanol intake using continuous and limited access two-bottle choice drinking tests in C57BL/6J mice. In both tests, TPCA-1 and sulfasalazine reduced ethanol intake and preference without changing total fluid intake or sweet taste preference. A virus expressing *Cre* recombinase was injected into the nucleus accumbens and central amygdala to selectively knockdown IKKβ in mice genetically engineered with a conditional *Ikkβ* deletion ($Ikk\beta^{F/F}$). Although IKKβ was inhibited to some extent in astrocytes and microglia, neurons were a primary cellular target. Deletion of IKKβ in either brain region reduced ethanol intake and preference in the continuous access two-bottle choice test without altering preference for sucrose. Pharmacological and genetic inhibition of IKKβ decreased voluntary ethanol consumption, providing initial support for IKKβ as a potential therapeutic target for alcohol abuse.

Keywords: Alcohol, Neurons, Astrocytes, Microglia, TPCA-1, Sulfasalazine, *Cre* recombinase, Nucleus accumbens, Central amygdala, DID, Binge drinking

Significance Statement

Alcoholism is a devastating disease with few pharmacological treatment options. The disease pathophysiology is unknown, but it is increasingly evident that proinflammatory signaling plays a role. NF-κB is a transcription factor that controls the expression of genes that are involved in inflammation and immunity. IKKβ mediates numerous inflammatory pathways and is responsible for disinhibiting NF-κB. The role of IKKβ in alcohol drinking had not previously been investigated. Our goal was to assess the peripheral and central effects of IKKβ on chronic and binge-like alcohol consumption and its potential role as a therapeutic target to reduce drinking.

Introduction

Alcohol exposure is known to activate peripheral and central proinflammatory pathways (Robinson et al., 2014; Crews and Vetreno, 2016). Genomic evidence for alcohol-induced inflammatory- and immune-related signaling comes from genetic association studies in alcoholics (Pastor et al., 2000; Pastor et al., 2005; Edenberg et al., 2008; Saiz et al., 2009), gene expression microarray studies in postmortem brains of alcoholics (Liu et al., 2006; Ökvist et al., 2007), and transcriptome meta-analyses in selectively bred (Mulligan et al., 2006) and ethanol-exposed mice (Gorini et al., 2013b2013a; Nunez et al., 2013; Osterndorff-Kahanek et al., 2013). Behavioral validation studies showed that mice with null mutations of different immune-related genes drank less ethanol (Blednov et al., 2012), while stimulation of innate immune responses using lipopolysaccharide produced prolonged increases in drinking (Blednov et al., 2011). Many of the inflammatory-related genes implicated in these studies mediate their effects through NF-κB.

NF-κB transcription family members are ubiquitously expressed throughout the body and play important roles in innate/adaptive immunity, cell death, and inflammation (Scheidereit, 2006; Perkins, 2007). NF-κB activation requires degradation of IκB, which occurs when the inhibitory kappa-B kinase (IKK) complex (composed of IKKα, IKKβ, and two IKKγ accessory molecules) phosphorylates serine residues in IκB, ultimately causing its degradation. NF-κB is subsequently released, where it translocates to the nucleus and acts as a transcription factor for numerous proinflammatory chemokines/cytokines, such as TNF-α and IL-6 (Schmid and Birbach, 2008; Gamble et al., 2012). The IKK complex represents a point of convergence for many inflammatory extracellular signals and plays a key role in inflammation and disease (Schmid and Birbach, 2008; Gamble et al., 2012). IKKβ specifically mediates the NF-κB classical pathway (Schmid and Birbach, 2008), has a clearly established role as an intermediate in NF-κB-induced cellular inflammation, and is involved in many inflammatory diseases (Grivennikov et al., 2010; Sunami et al., 2012).

Studies that have examined the effects of ethanol on IKKβ focused on peripheral effects, such as exacerbation of pancreatic and hepatic inflammation by chronic ethanol (Sunami et al., 2012; Huang et al., 2015). Studies of central actions of IKKβ have concentrated on neurodegenerative or metabolic disorders, but did not involve ethanol exposure (Zhang et al., 2008; Maqbool et al., 2013). Other studies have shown that IKKβ gene expression was altered in postmortem prefrontal cortex (PFC) from alcoholics (Flatscher-Bader et al., 2005) and mouse PFC following ethanol exposure and in selectively bred animals predisposed to drink alcohol (Mulligan et al., 2006; Osterndorff-Kahanek et al., 2015). To date, no studies have explored the peripheral or central effects of IKKβ on ethanol drinking. IKKβ is a compelling target for study given its role in inflammatory diseases and its role in mediating cocaine sensitization and reward through plasticity-dependent neuronal signaling in the nucleus accumbens (NAc) (Russo et al., 2009). Furthermore, IKKβ mediated the pro-depressant and anxiogenic effects of chronic stress through neuronal plasticity mechanisms in the NAc (Christoffel et al., 2011; Christoffel et al., 2012).

We examined different methods (pharmacological and genetic) to inhibit IKKβ, different brain regions/cell types, and different two-bottle choice (2BC) ethanol drinking paradigms in mice. Two different peripherally-acting IKKβ inhibitors, TPCA-1 and sulfasalazine, were tested in chronic and binge-like drinking models. TPCA-1 is a selective small molecule inhibitor of IKKβ (Podolin et al., 2005). Sulfasalazine does not cross the blood brain barrier (BBB) (Liu et al., 2012), possesses strong IKKβ inhibitory activity, and is used to treat inflammatory bowel disease, ulcerative colitis, and Crohn's disease (Lappas et al., 2005). We then examined the effects of *Cre*-mediated IKKβ knockdown in different cell types in the NAc or central amygdala (CeA) on voluntary ethanol consumption. Based on previous studies (Blednov et al., 2011; 2012), we hypothesized that inhibition of IKKβ would decrease proinflammatory signaling and reduce alcohol drinking.

Materials and Methods

Animals. Pharmacological antagonist studies were conducted in adult male C57BL/6J mice (original breeders were purchased from Jackson Laboratories, Bar Harbor, ME). Genetic knockdown studies were performed in adult male mice with a floxed *Ikkβ* gene on a C57BL/6J background (i.e., C57BL/6J mice with *Ikkβ* flanked by LoxP sites or more commonly denoted as $Ikk\beta^{F/F}$). Original breeders were acquired from Casey W. Wright, College of Pharmacy, The University of Texas at Austin. The C57BL/6J strain was chosen because of its propensity for voluntary ethanol consumption (Belknap et al., 1997). Mice were group-housed 4 or 5 per cage on a 12 h light/12 h dark cycle (lights on at 7:00 a.m.) with ad libitum access to water and rodent chow (Prolab RMH 180 5LL2 chow, TestDiet, Richmond, IN) in temperature- and humidity-controlled rooms. Behavioral testing began when the mice were at least 2 months old. Mice were individually housed at least 2 weeks before beginning the drinking tests. Experiments were conducted in isolated behavioral testing rooms in the Animal Resources Center at The University of Texas at Austin. All experiments were approved by the university's Institute for Animal Care and Use Committee and conducted in accordance with NIH guidelines with regard to the use of animals in research.

Pharmacological Inhibitors of IKKβ. Sulfasalazine (Sigma-Aldrich, St. Louis, MO) was injected i.p., and TPCA-1, 2-[(aminocarbonyl) amino]-5-(4-fluorophenyl)-3-thiophenecarboxamide (Tocris Bioscience, Minneapolis, MN), was administered p.o. Both drugs were freshly prepared as suspensions in saline with 4-5 drops of Tween-80 and injected in a volume of 0.1ml/10 g of body weight for i.p. administration, and 0.05 ml/10 g of body weight for oral administration. Drugs were administered 30 min prior to ethanol presentation times (see below). Doses of drugs and routes of administration were based on published data that showed anti-inflammatory activity *in vivo*.

Brain Region-Specific Lentiviral-Mediated Knockdown of IKKβ. *Ikkβ*$^{F/F}$ mice were injected bilaterally (into the NAc or CeA) with either a vesicular stomatitis virus (VSV-G) pseudotyped lentivirus expressing *Cre* recombinase fused to enhanced green fluorescent protein (EGFP) under the control of a CMV promoter (LV-Cre-EGFP) or an "empty" VSV-G pseudotyped lentiviral vector expressing only the EGFP transgene under a CMV promoter. Mice were anesthetized by isoflurane inhalation, placed in a model 1900 stereotaxic apparatus (David Kopf, Tujunga, CA), and administered preoperative analgesic (Rimadyl, 5 mg/kg). The skull was exposed, and bregma and lambda visualized with a dissecting microscope. A digitizer attached to the micromanipulator of the stereotaxic apparatus was used to locate coordinates relative to bregma. Burr holes were drilled bilaterally above the injection sites in the skull using a drill equipped with a #75 carbide bit (David Kopf, Tujunga, CA). The injection sites targeted either the NAc, using the following coordinates relative to bregma: anteroposterior (AP) +1.49 mm, mediolateral (ML) ±0.9 mm, dorsoventral (DV) -4.8 mm, or the CeA using the following coordinates: AP -1.14 mm, ML ±2.84 mm, DV -4.8 mm. Injections were performed using a Hamilton 10-µL microsyringe (model #1701) and a 30-gauge needle. The needle of the syringe was lowered to the DV coordinate and retracted 0.2 mm. Virus solutions (1.0 µL with titer of 1.8 x 10^8 vp/mL in PBS) were injected into each site at a rate of 200 nL/min. After each injection, the syringe was left in place for 5 min before being retracted over a period of 3 min. Incisions were closed with tissue adhesive (Vetbond, 3 M; St. Paul, MN). Mice were individually housed after surgery and given a 4-week recovery before starting the ethanol drinking tests.

Behavioral Testing. Three different ethanol drinking models were used in this study: 1) continuous 24-h 2BC with access to water and ethanol (15%, v/v), 2) 2BC drinking-in-the-dark (DID) with limited 3-h access to 15% ethanol (2BC-DID), and 3) 2BC using ascending concentrations of ethanol solutions (3-16%) (see below).

Pharmacological inhibitors of IKKβ. The effects IKKβ antagonists on ethanol intake were measured in adult male C57BL/6J mice in two different drinking paradigms: 2BC with 15% ethanol and 2BC-DID per protocols previously described (Blednov et al., 2003; 2014). For both tests, mice were pre-trained to consume 15% ethanol for at least 3 weeks to provide stable consumption. Ethanol intake was measured after saline injection (i.p. or p.o., corresponding to the route of administration for the antagonists) for 2 days and mice were grouped to provide similar levels of ethanol intake and preference. In the 2BC test, measurements of ethanol intake were made 6 and 24 h after beginning the drinking test, which began immediately after lights off. In the 2BC-DID test, drinking began 3 h after lights off and lasted for 3 h. Ethanol intake was measured once at the end of the 3-h drinking period. The position of the drinking tubes was changed daily to control for side preferences. Mice were weighed every 4 days. For both experiments, ethanol consumption (g/kg), preference (ratio of alcohol consumption to total fluid consumption), and total fluid intake (g/kg) were measured at the appropriate time points.

Brain region-specific lentiviral-mediated knockdown of IKKβ. The effects IKKβ knockdown in NAc and CeA on ethanol consumption were measured in adult male *Ikkβ*$^{F/F}$ mice using the 2BC test. Mice treated with either LV-Cre-EGFP or LV-EGFP-Empty 24-h were given continuous access to water and ascending concentrations of ethanol solutions (3%, 6%, 8%, 10%, 12%, 14%, 16% v/v) at 2-day intervals (Blednov et al., 2014). The position of administration tubes was changed daily to control for position preferences. Mice were weighed every 4 days. Ethanol consumption, preference, and total fluid intake were measured after 24 h.

Preference for saccharin. One month after completion of the 2BC ethanol test described above, *Ikkβ*$^{F/F}$ mice were tested for saccharin preference using the 2BC protocol. Mice were offered saccharin in increasing concentrations (0.008%, 0.016%, and 0.033%) and 24-h intake was calculated. Each concentration was offered for 2 days, and bottle positions were changed daily. The low concentration was presented first, followed by the higher concentrations.

RNA Isolation. After completion of behavioral testing, mice were killed by cervical dislocation and decapitated. The brains were quickly removed, flash frozen in liquid nitrogen, and later embedded in Optimal Cutting Temperature (OCT) media in isopentane on dry ice. Brains were then stored at −80° C for future processing. Brains were transferred to a cryostat set at −6°C for at least 1 h before sectioning. Sections (300 µm) were collected from +1.80 to +0.60 mm (AP) relative to bregma and transferred to pre-cooled glass slides on dry ice. Micropunch sampling was performed on a frozen stage (−25°C) using Dual Fluorescent Protein Flashlight (Nightsea, Bedford, MA), and a mouse stereotaxic atlas to identify the GFP expression and anatomical location of the injection site. Microdissection punches (Stoelting Co., Wood Dale, IL) with an inner diameter of 0.75 mm were used to obtain samples of NAc. This inner diameter fit within the viral spread around the injection site and minimized contamination from other tissue. Punches were taken bilaterally from 4-300-µm sections and stored at −80°C until RNA extraction. Micropunches were washed with 100% ethanol and RNaseZap (Life Technologies, Carlsbad, CA) between each animal. All equipment used to obtain tissue was treated with RNaseZap (Life Technologies) to prevent RNA degradation. Total RNA was extracted using the MagMAX™-96 for Microarrays Total RNA Isolation Kit (Life Technologies) according to the manufacturer's instructions. RNA yields and purity were assessed using a NanoDrop 8000 (Thermo Fisher Scientific, Waltham, MA). Both the 260/230 and 260/280 ratios were >2.0. RNA quality was determined using the Agilent 2200 TapeStation (Agilent, Santa Clara, CA) with RNA integrity numbers (RIN) averaging above 8.0.

Quantitative PCR. To verify *Ikkβ* mRNA knockdown, single-stranded cDNA was synthesized from total RNA using the TaqMan® High Capacity RNA-to-cDNA kit (Life Technologies). Following reverse transcription, quantitative real-time PCR (qPCR) was performed in triplicate using TaqMan® Gene Expression Assays together with the TaqMan® Gene Expression Master Mix (Life Technologies), per manufacturer's instructions. TaqMan® Gene Expression assays

used were *Ikbkb* (ID: Mm01222247_m1), *Tnf-α* (ID: Mm00443258_m1), *Il-6* (ID: Mm00446190_m1), and Enhanced GFP (ID: Mr04097229_mr). *Gapdh* (Mm99999915_g1) (glyceraldehyde-3-phosphate dehydrogenase) was used as a reference gene, and relative mRNA levels were determined using the $2^{-\Delta\Delta CT}$ method (Schmittgen and Livak, 2008). *Gapdh* was used as the endogenous control because of its low variability between samples. Reactions were carried out in a CFX384™ Real-Time PCR Detection System (Bio-Rad, Hercules/California) and data collected using Bio-Rad CFX Manger. All genes were normalized to the endogenous housekeeping gene, *Gapdh*, and expressed relative to the respective LV-EGFP-Empty control treatment.

Immunohistochemistry.

Tissue harvesting. Animals were killed, transcardially perfused with Phosphate Buffer Saline (PBS) and 4% paraformaldehyde (PFA), and brains were harvested, postfixed for 24 h in 4% PFA at 4°C, and cyroprotected for 24 h in 20% sucrose in PBS at 4°C. Brains were placed in molds containing OCT compound (VWR, Radnor, PA) and frozen in isopentane on dry ice. The brains were equilibrated in a -12 to -14°C cryostat (Thermo Fischer Scientific) for at least 1 h and coronal sections of 30 µm were taken from the NAc and CeA and placed in sterile PBS.

Immunostaining. Sections were penetrated with 0.1% Triton-X 100 (2 x 10 min at 25°C), washed in PBS (3 x 5 min at 25°C), blocked with 10% goat or donkey serum (30 min at 25°C), and treated with 1:250 anti-IKKβ (Millipore, Billerica, MA), 1:500 anti-NeuN (Santa Cruz, Santa Cruz, CA), 1:300 anti-GFAP (Santa Cruz), 1:1000 anti-Iba1 (Dako, Dako, Denmark), and 1:1000 anti-GFP (Santa Cruz) antibodies (4°C overnight), washed in PBS (3 x 10 min at 25°C), and then subjected to reaction with fluorescence-conjugated secondary antibodies of 1:1000 Alexa 488 and 1:1000 Alexa 568 (Invitrogen, Waltham, MA) (2 h at 25°C), and rinsed with PBS (3 x 10 min at 25°C). The sections were mounted on slides using sterile 0.2% gelatin and DAPI

mounting media (Vector Laboratories, Burlingame, CA) and cover slipped. Images were taken using either a Zeiss Axiovert 200M Fluorescent Microscope (Zeiss, Oberkocheen, Germany) equipped with a 20x objective or a Zeiss LSM 710 Confocal Microscope (Zeiss) equipped with a 63x objective. For the immunohistochemistry, two sets of control experiments were performed to test specificity: 1) replacement of the primary antibody with only the serum of the appropriate species and 2) omission of secondary antibodies. No immunostaining was detected under either of these conditions.

Target verification. Serial sections (30 µm) of NAc (AP +2.00 to 0.00 mm) and CeA (AP 0.00 to -2.00 mm) were mounted on slides with DAPI mounting media (Vector Laboratories) and visualized using a Zeiss Axiovert 200M Fluorescent Microscope (Zeiss) equipped with a 10x objective to assess the location of the injection site. The quality of injection was quantitatively scored based of the strength of EGFP viral expression, injection location relative to target, and the spread of the virus. The injection was considered on target if the needle placement was within 0.3 mm of the desired stereotaxic coordinates and the virus EGFP expression covered at least 1/3 of the brain region of interest (i.e., NAc, CeA) on at least one side of the brain.

Image analysis. Brain sections were prepared as described in the Immunohistochemistry methods. Epi-fluorescent images were acquired using a Zeiss Axiovert 200M Fluorescent Microscope (Zeiss) equipped with a 20x objective and an automated stage. Images of the brain region of interest were captured (multiple 20x images in red, green, and blue channels) then stitched together creating a composite view for further analysis. Images were taken without saturating the signal and digitized at 8-bits using the full intensity range of 0–256, and imported into the ImageJ software package (http://imagej.nih.gov/ij/). Composite images were split into individual channels, overlaid with a grid, and colocalized cells were counted. A Zeiss LSM 710 Confocal Microscope (Zeiss) equipped with a 63x objective was used to take representative images for IKKβ cell-type specificity viral trophism.

Statistical Analysis. Numerical data are shown as mean ± SEM, and n represents the number of animals tested. Data were analyzed using either analysis of variance (ANOVA) with repeated measures followed by Bonferroni post hoc tests or Student's t-tests as appropriate (GraphPad Software, Inc., La Jolla, CA). Calculated p-values < 0.05 were considered statistically significant.

Results

Pharmacological inhibitors of IKKβ reduce ethanol consumption and preference in the continuous 24-h 2BC test. We first investigated the effects of systemic IKKβ inhibition on voluntary ethanol drinking. A pharmacological approach was selected because IKKβ genetic deficiency causes embryonic lethality due to liver degeneration and apoptosis (Tanaka et al., 1999). Low and high doses of TPCA-1 or sulfasalazine were administered to adult male C57BL/6J mice on a daily basis. Voluntary ethanol (15%) drinking was evaluated using a continuous 24-h 2BC test. The lower dose of TPCA-1 (30 mg/kg) did not significantly alter ethanol intake, but the higher dose (50 mg/kg) reduced ethanol intake [$F(1,18) = 6.9$, $p<0.05$] and preference [$F(1,18) = 8.3$, $p<0.01$] 6 h after administration (Figures 1 A and B). Both doses of sulfasalazine reduced ethanol intake [Student's t-test, $p<0.05$ and $F(1,10) = 24.1$, $p<0.001$, respectively] and preference [Student's t-test, $p<0.05$ and $F(1,10) = 12.4$ $p<0.01$, respectively] (Figures 1 D and E). No changes in total fluid intake were observed after administration of either drug (Figures 1 C and F). There were no differences in ethanol intake or preference between drug- and saline-treated groups 18 h post-treatment for either drug (data not shown).

Pharmacological inhibitors of IKKβ reduce ethanol consumption and preference in the limited-access drinking-in-the-dark (DID) 2BC test. We administered TPCA-1 (50 mg/kg) or sulfasalazine (100 mg/kg) daily to a different cohort of adult male C57BL/6J mice and performed a 2BC test with limited 3-h access to 15% ethanol during the dark phase of the light/dark cycle,

296 referred to as the 2BC-DID test. Compared to the continuous 2BC test, the 2BC-DID paradigm
297 more closely replicates binge drinking, where mice typically consume higher levels of ethanol
298 and exhibit behavioral evidence of intoxication (Thiele and Navarro, 2014). In this model, TPCA-
299 1 reduced ethanol consumption [$F(1,10) = 14.0$, $p<0.01$] and preference [$F(1,10) = 21.6$, $p<0.01$]
300 without affecting total fluid intake (Figures 2 A-C). Sulfasalazine, however, did not significantly
301 alter ethanol or total fluid intake, but did reduce ethanol preference [$F(1,14) = 31.7$, $p<0.001$]
302 (Figures 2 D-F). There was a significant interaction between treatment and time of ethanol
303 consumption with a gradual time-dependent decrease in the effect of sulfasalazine (Figure 2 D).
304
305 **Brain region-specific knockdown of IKKβ in the NAc or CeA reduces ethanol**
306 **consumption and preference in the continuous 24-h 2BC test.** We next examined the role
307 of IKKβ in two key areas of the brain implicated in the pathogenesis of alcohol use disorder
308 (AUD). The NAc was chosen because it is part of the mesolimbic dopamine reward system that
309 positively reinforces addictive behavior (Koob and Volkow, 2010; Koob, 2014). The NAc has
310 also been implicated in IKKβ-mediated rewarding effects of cocaine (Russo et al., 2009). The
311 CeA was selected because it is in involved in activating brain stress systems through the
312 release of corticotropin-releasing factor and it negatively reinforces addictive behaviors (Koob
313 and Le Moal, 2008; Koob and Volkow, 2010; Koob, 2014). Mice genetically engineered with a
314 conditional *Ikkβ* deletion ($Ikk\beta^{F/F}$) were injected bilaterally in the brain region of interest with a
315 lentivirus expressing either *Cre* fused to EGFP (LV-EGFP-Cre) or only EGFP (LV-EGFP-
316 Empty). The transgenes of both viral vectors were under the control of a cytomegalovirus (CMV)
317 promoter and were pseudotyped with vesicular stomatitis virus glycoprotein (VSV-G).
318 Expression of *Cre* results in the excision of *Ikkβ*. This method of targeted IKKβ deletion was
319 validated by injecting LV-EGFP-Cre (n=8) and LV-EGFP-Empty (n=8) in the NAc of adult male
320 $Ikk\beta^{F/F}$ mice followed by a 3- or 8-week incubation period. The time points were selected based
321 on previous work in mouse brain showing maximal changes in expression 2 to 4 weeks post-

322 injection (Ahmed et al., 2004). In addition, the 3- and 8-week post-injection time points were
323 chosen to assess the level of IKKβ knockdown near the beginning (4 weeks post-injection) and
324 end (8 weeks post-injection) of the drinking studies. At the appropriate time points, brains were
325 perfused, harvested, sectioned, and immunostained with anti-IKKβ and anti-EGFP. The number
326 of cells with the viral EGFP that colocalized with IKKβ were measured and compared between
327 the LV-EGFP-Cre and LV-EGFP-Empty treatments at each time point. The relative expression
328 of IKKβ in Cre-treated animals vs. controls was 0.596 ± 0.012 ($p<0.01$) at 3 weeks and 0.099 ±
329 0.023 ($p<0.001$) at 8 weeks (Figure 3). These represent a 40% and 90% decrease in IKKβ after
330 3 and 8 weeks, respectively.
331 Subsequently, *Ikkβ*$^{F/F}$ mice were injected bilaterally with LV-EGFP-Cre or LV-EGFP-
332 Empty into either the NAc or CeA. After 4 weeks, the 2BC drinking test was administered in
333 which mice could drink either water or a series of increasing ethanol concentrations ranging
334 from 3 to 16%. Similar to the results after peripheral inhibition of IKKβ, targeted deletion of IKKβ
335 in the NAc also reduced ethanol consumption [$F(1, 50) = 10.0$, $p<0.005$] and preference [$F(1,$
336 $50) = 8.3$, $p<0.01$] without affecting total fluid intake (Figures 4 A-C). Likewise, local deletion of
337 IKKβ in the CeA reduced ethanol consumption [$F(1,196) = 19.1$, $p<0.0001$] and preference
338 [$F(1,196) = 23.9$, $p<0.0001$] with no change in total fluid intake (Figures 5 A-C). At the higher
339 ethanol concentrations, consumption and preference were reduced by greater than 40% and
340 25%, respectively, after targeted knockdown in both regions (Figures 4 and 5).
341 Because ethanol drinking behavior in the 2BC test depends partly on taste (Bachmanov
342 et al., 2003), we investigated the effect of the lentiviral-mediated knockdown of IKKβ in the NAc
343 and CeA on preference for sweet/noncaloric (saccharin) solutions. After the ethanol drinking
344 experiments, we administered a 2BC test using three different concentrations of saccharin
345 versus water. Analysis of preference for saccharin indicated a significant main effect of
346 concentration in both the NAc [$F(2,56) = 69.97$, $p<0.0001$] and CeA [$F(2,56) = 53.43$, $p<0.0001$],
347 but no effect of treatment (LV-EGFP-Cre, LV-EGFP-Empty) or treatment × concentration

interaction (Figures 6A and 7C, respectively). Analysis of total fluid intake revealed no significant differences between the LV-EGFP-Cre and LV-EGFP treatment groups (Figures 6B and 7D). Thus, knockdown of IKKβ in either the NAc or CeA did not change preference for saccharin.

Upon completion of the behavioral experiments (~8 weeks post-injection), knockdown of IKKβ in the NAc and CeA was verified by 1) anatomical assessment of needle placement and viral spread, 2) confirmation of IKKβ protein knockdown, and 3) exploration of changes in mRNA levels of *Ikkβ* and downstream proinflammatory cytokines in the NF-κB canonical pathway. To assess needle placement and viral spread, animals were perfused and brains harvested from a subset of the lentiviral-treated $Ikk\beta^{F/F}$ mice used in the brain region-specific IKKβ knockdown experiments (NAc: n=22 LV-EGFP-Cre, n=14 LV-EGFP-Empty; CeA: n=15 LV-EGFP-Cre, n=5 LV-EGFP-Empty). Injection coordinates and coverage of the NAc and CeA were verified using immunofluorescence to detect EGFP. Figures 7A and C are representative images of coronal sections in the NAc [Anterior Posterior (AP) +1.49 mm] and CeA (AP -1.14 mm), respectively, of the $Ikk\beta^{F/F}$ mice treated with either LV-EGFP-Cre or LV-EGFP-Empty. The left side of the fluorescent image shows the EGFP signal (surrogate marker for lentiviral transduction) in green and DAPI (a stain that visualizes the nuclei of all cells) in blue. The right side of the image is a brightfield image used to better visualize the neuroanatomical landmarks. Figures 7C and D are coronal sections from a mouse brain atlas in the area of the desired target coordinates with the blue circles showing the NAc and CeA and the green ovals demonstrating the typical area where the LV-EGFP-Cre and LV-EGFP-Empty treatments transduced. After completion of the drinking tests, analysis of brain sections from knockdowns in NAc and CeA revealed that 100% of the samples met the criteria of 1) needle placement in at least one side within ± 0.3 mm of the desired stereotaxic coordinates, and 2) viral expression coverage that was greater than 1/3 of the area in the brain region of interest. The average viral coverage per injection site as indicated by the EGFP signal was 37.8% ± 4.8 in the NAc and 50.9% ± 5.7 in the CeA (mean ± SEM).

After the 2BC drinking tests, IKKβ protein knockdown was confirmed in a subset of mice from the NAc and CeA experiments using immunohistochemistry (n=5 LV-EGFP-Cre and n=5 LV-EGFP-Empty for each experiment). Brains were prepared, immunostained, and analyzed in the same manner as the IKKβ knockdown experiment (after 3 and 8 weeks) previously described. The relative expression of IKKβ in Cre-treated animals vs. control was 0.122 ± 0.026 ($p<0.001$) in the NAc and 0.141 ± 0.028 ($p<0.001$) in the CeA (mean ± SEM) (Figure 8A). These represent an 88% and 86% decrease in the NAc and CeA, respectively. These results were consistent with those obtained in pilot IKKβ knockdown experiments 8-weeks post-injection.

To determine changes in mRNA levels of *Ikkβ* and downstream cytokines in the NF-κB canonical pathway, we performed quantitative PCR on micropunches from the NAc and CeA. A subset of slices from NAc (n=10 LV-EGFP-Cre, n=6 LV-EGFP-Empty) and CeA (n=5 LV-EGFP-Cre, n=5 LV-EGFP-Empty) experiments were harvested, flash frozen, sectioned, and micropunches were collected at the injection site. The relative expression of *Ikkβ* was 0.321 ± 0.049 ($p<0.001$) in the NAc and 0.360 ± 0.056 ($p<0.001$) in the CeA; *Tnf* expression was 0.568 ± 0.059 ($p<0.01$) in the NAc and 0.488 ± 0.084 ($p<0.01$) in the CeA; and *Il6* expression was 0.595 ± 0.055 ($p<0.01$) in the NAc and 0.641 ± 0.060 ($p<0.01$) in the CeA (mean ± SEM). These values indicate approximately 68% and 64% decrease in *Ikkβ* mRNA in the NAc and CeA, respectively, and 35% or greater knockdown of *Tnf* and *Il6* mRNA in both brain regions (Figure 8).

IKKβ was expressed primarily in neurons in the NAc and CeA. To further investigate IKKβ's specificity in these regions, we determined the cell-type localization of IKKβ in the NAc and CeA. Brain slices were co-stained using antibodies against IKKβ and three common cell-type markers in the brain (neurons: anti-NeuN; astrocytes: anti-GFAP; microglia: anti-Iba1) from three adult male alcohol-naive C57BL/6J mice. Using fluorescent light microcopy to visualize

399 IKKβ signal colocalization, we observed that in both the NAc and CeA, IKKβ was expressed in
400 all three cell types to some degree, but was primarily expressed in neurons (Figure 9).
401 Subsequently, we examined the trophism of the viral vector delivery system by co-
402 staining brain slices from LV-EGFP-Cre treated animals in the NAc and CeA (n=2 NAc LV-
403 EGFP-Cre, n=2 CeA LV-EGFP-Cre) using an antibody to target EGFP and the same three cell-
404 specific markers described above. EGFP under the control of a CMV promoter in the VSV-G
405 pseudotyped lentiviral vectors was expressed primarily in neurons (74.6% ± 1.3%), slightly in
406 astrocytes (10.8% ± 2.2%), and only marginally in microglia (1.8% ± 0.5%) (Figure 10).
407
408 **Identification of *Nfkb* targets.** We previously examined chronic ethanol-induced changes in
409 gene expression patterns in mouse brain (Osterndorff-Kahanek et al., 2015) and used these
410 datasets to determine changes in downstream *Nfkb/Rel* gene targets in mouse CeA, NAc, and
411 PFC. Ingenuity Pathway Analysis was used to curate and identify potential gene targets in mice
412 and humans. As shown in Table 1, we identified numerous targets, suggesting that large
413 networks of downstream genes may be altered by ethanol. Ethanol has also been shown to
414 alter gene expression of IKKβ in mice (Osterndorff-Kahanek et al., 2015) and humans
415 (Flatscher-Bader et al., 2005; Mayfield et al., unpublished), and IKKβ may represent an
416 upstream intermediate target to control NF-κB activation and reduce alcohol-induced changes in
417 gene expression.
418
419 **Discussion**
420 IKKβ is a critical component in the regulation of the NF-κB inflammatory cascade, but its
421 role in alcohol drinking had not been investigated prior to this study. Inhibiting IKKβ either
422 peripherally, or in brain regions associated with addictive behaviors, decreased voluntary
423 ethanol consumption and preference in several drinking tests, including chronic and binge-like
424 paradigms. Systemic administration of the peripherally-acting IKKβ inhibitors, TPCA-1 or

sulfasalazine, reduced ethanol drinking in two distinct drinking models (2BC and 2BC-DID). The ability of sulfasalazine and TPCA-1 to penetrate the BBB is not well established, and their anti-inflammatory effects are thought to be confined to the periphery (Liu et al., 2012). However, it is possible that inhibition of systemic inflammatory signaling during chronic drinking also impacts central pathways. Decreased levels of proinflammatory cytokines in blood, for example, could translate to decreased cytokine release and signaling across the BBB, ultimately decreasing levels of inflammatory mediators in brain. We also note that other anti-inflammatory agents, such as minocycline, were proposed to reduce drinking in mice through direct central actions (Agrawal et al., 2014). It has been hypothesized that alcohol-induced inflammatory responses signal via peripheral-central positive feedback cycles (Robinson et al., 2014). Regardless of the primary mechanism, the ability of peripheral IKKβ inhibitors to successfully inhibit chronic and binge-like drinking alludes to their translational potential as a therapeutic target.

Knockdown of IKKβ in the NAc or CeA was sufficient to decrease voluntary 2BC ethanol consumption, showing that drinking behavior can be selectively regulated by IKKβ's central actions. The NAc is part of the mesolimbic dopamine reward system, which has a well-documented role in substance abuse, and has also been implicated in the rewarding effects of cocaine mediated by IKKβ (Russo et al., 2009). The CeA is involved in fear-motivated behaviors associated with drug and alcohol abuse and has been shown to mediate the behavioral effects of acute and chronic ethanol consumption in rodents (Roberto et al., 2004a; Roberto et al., 2004b; Roberto et al., 2006; Lam et al., 2008). Lesions of the central, but not basolateral, amygdala decreased voluntary ethanol consumption (Moller et al., 1997), and a review of the neurocircuitry of drug addiction further highlights the role of plasticity in frontal cortical and subregions of the amygdala in craving, withdrawal, negative affect, and loss of control (Koob and Volkow, 2010). Thus, the brain regions targeted here have key roles in alcohol addiction-mediated behaviors and were both sensitive to IKKβ knockdown.

We provide initial evidence that IKKβ knockdown disrupts proinflammatory cascades in the NAc and CeA based on decreased expression of downstream products of the NF-κB canonical pathway (TNF-α and IL-6) in both regions. Although the corresponding reductions in these inflammatory cytokines suggest that this pathway is responsible for the decreased drinking, these results do not provide specific mechanistic evidence of downstream effects. Other studies have hypothesized that alcohol-induced increases in levels of cytokines promote excessive alcohol consumption in animal models and human alcoholics (Blednov et al., 2011; Robinson et al., 2014). This may in turn exacerbate inflammatory responses via activation of NF-κB. In fact, NF-κB DNA binding in the brain has been shown to increase with ethanol treatment (Crews et al., 2006) and the human *NFKB1* gene has also been linked with alcoholism (Edenberg et al., 2008).

In addition, previous evidence suggests that chronic ethanol alters gene expression of IKKβ in mouse PFC (Osterndorff-Kahanek et al., 2015) and human postmortem PFC from alcoholics (Flatscher-Bader et al., 2005). Furthermore, our current evidence suggests that NF-κB-related gene targets are ethanol-responsive in mouse CeA, NAc, and PFC, potentially affecting a significant number of downstream targets (mouse and human). Based on the genomic evidence in mice and humans and the many networks of downstream genes that may be dysregulated, ethanol-mediated changes in IKKβ regulation of NF-κB cascades are relevant targets that may offer new treatment strategies for AUD.

In addition to different brain regions, different cell types may play unique roles in inflammatory responses (Szabo and Lippai, 2014; Lacagnina et al., 2016; Warden et al., 2016). Inflammatory pathways are not limited to glia or other immunocompetent cells, but also involve neurons and neuronal-glial interactions. In our study, the selective knockdown of IKKβ did not affect all cell types equally, due in part to the viral delivery system. IKKβ was expressed primarily in neurons in the NAc and CeA with lessor amounts found in glia (e.g., astrocytes and microglia). The cell-type specificity of the viral vector system delivering *Cre* favored the

transduction in neurons, and to a lesser degree in astrocytes, and only marginally in microglia. Even though IKKβ was knocked down to some extent in all three cell types, neurons appear to be a primary target. Because GFAP only labels a subset of astrocytes in the CNS and is not an ideal marker, our estimation that IKKβ knockdown occurred in only 10% of astrocytes may be an underestimation. While this caveat warrants the consideration of the role of IKKβ in astrocytes, it does not detract from the novel evidence that neurons are involved in the IKKβ-mediated reduction in ethanol drinking.

The IKK complex (IKKα, IKKβ, and IKKγ) is a crucial mediator for several proinflammatory pathways that ultimately result in the activation of the NF-κB canonical pathway. Specifically, IKKβ primarily regulates the NF-κB canonical pathway (transcription of inflammatory genes/anti-apoptosis), IKKα regulates the NF-κB non-canonical pathway (cell cycle regulation/proliferation), while IKKγ participates in both pathways (Perkins, 2007; Gamble et al., 2012). We suggest that knockdown of IKKβ in the NAc and CeA targeted the canonical pathway in neurons and to some extent astrocytes, interrupting inflammatory signaling and feedback cycles.

The central effects of IKKβ are not well known, and prior to this work its role in alcohol drinking had not been investigated. Our results provide novel evidence that peripheral and/or central inhibition of IKKβ decreases ethanol drinking, including binge-like consumption. Alcohol could induce peripheral cytokines that ultimately activate expression of immune-related genes in the brain or could directly stimulate central immune- and inflammatory-related pathways. Inhibiting IKKβ-mediated signaling could dampen the peripheral as well as the central inflammatory effects of ethanol. Our results are consistent with other studies showing that null mutant mice lacking genes associated with proinflammatory pathways had reduced levels of chemokines and cytokines and reduced voluntary ethanol consumption (Blednov et al., 2005; 2012). However, not all inflammatory-related genes studied to date have been shown to regulate ethanol drinking in mouse knockout models (Mayfield et al., 2016), suggesting that

indiscriminant inhibition of inflammatory pathways is not a viable strategy to limit excessive drinking and further highlighting the relevance of the current study in targeting treatment strategies.

In summary, voluntary ethanol drinking was decreased by inhibiting IKKβ peripherally using pharmacological inhibitors or centrally using genetic deletions in the CeA or NAc, regions known to be important in the neurobiology of alcohol abuse (Koob and Volkow, 2010). Although the effects of inflammatory pathways are often attributed to glia (astrocytes and microglia), this study highlights a novel neuronal role for IKKβ in alcohol consumption. Our results also provide evidence that the use of peripheral-acting IKKβ inhibitors with anti-inflammatory properties is a potential treatment strategy for decreasing alcohol drinking. In particular, drugs like sulfasalazine that are already FDA approved, may provide fast track treatment options for AUD or other inflammatory-related diseases. Studies such as this that probe key inflammatory pathways, peripheral-central components, different drinking models, and brain region- and cell type-specificity will continue to refine treatment strategies and opportunities for AUD.

517 **Table 1. Ethanol-induced changes in NFKB/REL gene targets in mouse brain.**

CeA		NAc		PFC	
Illumina Probe ID	**NFKB-REL Targets (IPA)**	**Illumina Probe ID**	**NFKB-REL Targets (IPA)**	**Illumina Probe ID**	**NFKB-REL Targets (IPA)**
ILMN_2738825	*ACTA1*	ILMN_2878060	*ANXA6*	ILMN_2878060	*ANXA6*
ILMN_2739999	*B2M*	ILMN_2739999	*B2M*	ILMN_1221503	*CCND1*
ILMN_1216746	*B2M*	ILMN_1216746	*B2M*	ILMN_2601471	*CCND1*
ILMN_2717613	*CDK2*	ILMN_2706514	*BCL2*	ILMN_2931411	*CCT3*
ILMN_2756435	*CEBPB*	ILMN_2716567	*BNIP3L*	ILMN_2846775	*CDKN1A*
ILMN_2609813	*CHI3L1*	ILMN_2756435	*CEBPB*	ILMN_2634083	*CDKN1A*
ILMN_1224754	*CKB*	ILMN_2959480	*EIF4A1*	ILMN_2846776	*CDKN1A*
ILMN_2747651	*HAT1*	ILMN_2718815	*FAF1*	ILMN_2992403	*CINP*
ILMN_2624153	*HES5*	ILMN_2994806	*H2AFJ*	ILMN_2627041	*CX3CL1*
ILMN_1253414	*HES5*	ILMN_2648292	*H3F3A/H3F3B*	ILMN_1256348	*DNTTIP1*
ILMN_2791952	*HES6*	ILMN_1253414	*HES5*	ILMN_2737713	*EDN1*
ILMN_1222313	*HIST1H4J*	ILMN_2791952	*HES6*	ILMN_2903945	*GADD45G*
ILMN_2924419	*HLA-A*	ILMN_2855315	*HIST1H1C*	ILMN_2791952	*HES6*
ILMN_2835683	*HLA-A*	ILMN_2924419	*HLA-A*	ILMN_2835683	*HLA-A*
ILMN_1235470	*HNRNPC*	ILMN_2835683	*HLA-A*	ILMN_3156604	*HMGB2*
ILMN_1239021	*HNRNPM*	ILMN_2715802	*HMGA1*	ILMN_2664319	*IRF3*
ILMN_2646625	*JUN*	ILMN_1235470	*HNRNPC*	ILMN_2646625	*JUN*
ILMN_2878071	*LYZ*	ILMN_2511051	*HNRNPC*	ILMN_3001914	*NFKBIA*
ILMN_2640883	*NDE1*	ILMN_2921103	*HNRNPM*	ILMN_2596979	*NRARP*
ILMN_2596979	*NRARP*	ILMN_2921095	*HNRNPM*	ILMN_3158919	*PRKCZ*
ILMN_1242466	*PSMB9*	ILMN_1239021	*HNRNPM*	ILMN_2647533	*SLC41A3*
ILMN_2717621	*RPS15A*	ILMN_2646625	*JUN*	ILMN_2938893	*SMAD3*
ILMN_2883164	*SERPINE2*	ILMN_1258376	*KCNK6*	ILMN_2701664	*TSC22D3*
ILMN_2701664	*TSC22D3*	ILMN_1258526	*LGALS3BP*	ILMN_3150811	*TSC22D3*
ILMN_3150811	*TSC22D3*	ILMN_2878071	*LYZ*	ILMN_3112873	*TXNIP*
ILMN_3121255	*VEGFA*	ILMN_2640883	*NDE1*		
		ILMN_2596979	*NRARP*		
		ILMN_2790181	*PHGDH*		
		ILMN_1234766	*PPME1*		
		ILMN_2833378	*PRKACA*		

		ILMN_1242466	*PSMB9*		
		ILMN_1248316	*PTGDS*		
		ILMN_2728729	*SDC4*		
		ILMN_3027751	*SORBS1*		
		ILMN_2988299	*SRF*		
		ILMN_2692615	*TGM2*		
		ILMN_2701664	*TSC22D3*		
		ILMN_3150811	*TSC22D3*		
		ILMN_3112873	*TXNIP*		

Ethanol administration produced numerous changes in NFKB/REL gene targets in mouse central amygdala (CeA), nucleus accumbens (NAc) and prefrontal cortex (PFC). Ingenuity Pathway Analysis was used to curate gene targets. Gene target identification included both human and mouse databases. Human nomenclature is used here. Adjusted p values are listed using an FDR of $p<0.001$. Experimental details are provided in Osterndorff-Kahanek et al., 2015.

References

Agrawal RG, Owen JA, Levin PS, Hewetson A, Berman AE, Franklin SR, Hogue RJ, Chen Y, Walz C, Colvard BD, Nguyen J, Velasquez O, Al-Hasan Y, Blednov YA, Fowler A-K, Syapin PJ, Bergeson SE (2014) Bioinformatics Analyses Reveals Age-Specific Neuroimmune Modulation as a Target for Treatment of High Ethanol Drinking. Alcoholism, clinical and experimental research 38:428-437.

Ahmed BY, Chakravarthy S, Eggers R, Hermens WT, Zhang JY, Niclou SP, Levelt C, Sablitzky F, Anderson PN, Lieberman AR, Verhaagen J (2004) Efficient delivery of Cre-recombinase to neurons in vivo and stable transduction of neurons using adeno-associated and lentiviral vectors. BMC neuroscience 5:4.

535 Bachmanov AA, Kiefer SW, Molina JC, Tordoff MG, Duffy VB, Bartoshuk LM, Mennella JA
536 (2003) Chemosensory factors influencing alcohol perception, preferences, and
537 consumption. Alcoholism, clinical and experimental research 27:220-231.
538 Belknap JK, Richards SP, O'Toole LA, Helms ML, Phillips TJ (1997) Short-Term Selective
539 Breeding as a Tool for QTL Mapping: Ethanol Preference Drinking in Mice. Behav Genet
540 27:55-66.
541 Blednov YA, Benavidez JM, Black M, Harris RA (2014) Inhibition of phosphodiesterase 4
542 reduces ethanol intake and preference in C57BL/6J mice. Frontiers in neuroscience 8:129.
543 Blednov YA, Walker D, Alva H, Creech K, Findlay G, Harris RA (2003) GABAA receptor alpha 1
544 and beta 2 subunit null mutant mice: behavioral responses to ethanol. J Pharmacol Exp
545 Ther 305:854-863.
546 Blednov YA, Bergeson SE, Walker D, Ferreira VM, Kuziel WA, Harris RA (2005) Perturbation of
547 chemokine networks by gene deletion alters the reinforcing actions of ethanol. Behavioural
548 brain research 165:110-125.
549 Blednov YA, Benavidez JM, Geil C, Perra S, Morikawa H, Harris RA (2011) Activation of
550 inflammatory signaling by lipopolysaccharide produces a prolonged increase of voluntary
551 alcohol intake in mice. Brain, behavior, and immunity 25 Suppl 1:S92-S105.
552 Blednov YA, Ponomarev I, Geil C, Bergeson S, Koob GF, Harris RA (2012) Neuroimmune
553 regulation of alcohol consumption: behavioral validation of genes obtained from genomic
554 studies. Addiction biology 17:108-120.
555 Christoffel DJ, Golden SA, Heshmati M, Graham A, Birnbaum S, Neve RL, Hodes GE, Russo
556 SJ (2012) Effects of inhibitor of kappaB kinase activity in the nucleus accumbens on
557 emotional behavior. Neuropsychopharmacology : official publication of the American College
558 of Neuropsychopharmacology 37:2615-2623.
559 Christoffel DJ, Golden SA, Dumitriu D, Robison AJ, Janssen WG, Ahn HF, Krishnan V, Reyes
560 CM, Han MH, Ables JL, Eisch AJ, Dietz DM, Ferguson D, Neve RL, Greengard P, Kim Y,

561 Morrison JH, Russo SJ (2011) IkappaB kinase regulates social defeat stress-induced
562 synaptic and behavioral plasticity. J Neurosci 31:314-321.
563 Crews F, Nixon K, Kim D, Joseph J, Shukitt-Hale B, Qin L, Zou J (2006) BHT blocks NF-kappaB
564 activation and ethanol-induced brain damage. Alcoholism, clinical and experimental
565 research 30:1938-1949.
566 Crews FT, Vetreno RP (2016) Mechanisms of neuroimmune gene induction in alcoholism.
567 Psychopharmacology 233:1543-1557.
568 Edenberg HJ, Xuei X, Wetherill LF, Bierut L, Bucholz K, Dick DM, Hesselbrock V, Kuperman S,
569 Porjesz B, Schuckit MA, Tischfield JA, Almasy LA, Nurnberger JI, Foroud T (2008)
570 Association of NFKB1, which encodes a subunit of the transcription factor NF-κB, with
571 alcohol dependence. Human Molecular Genetics 17:963-970.
572 Flatscher-Bader T, van der Brug M, Hwang JW, Gochee PA, Matsumoto I, Niwa S, Wilce PA
573 (2005) Alcohol-responsive genes in the frontal cortex and nucleus accumbens of human
574 alcoholics. J Neurochem 93:359-370.
575 Gamble C, McIntosh K, Scott R, Ho KH, Plevin R, Paul A (2012) Inhibitory kappa B Kinases as
576 targets for pharmacological regulation. Br J Pharmacol 165:802-819.
577 Gorini G, Roberts AJ, Mayfield RD (2013a) Neurobiological Signatures of Alcohol Dependence
578 Revealed by Protein Profiling. PLoS ONE 8:e82656.
579 Gorini G, Nunez YO, Mayfield RD (2013b) Integration of miRNA and Protein Profiling Reveals
580 Coordinated Neuroadaptations in the Alcohol-Dependent Mouse Brain. PLoS ONE
581 8:e82565.
582 Grivennikov SI, Greten FR, Karin M (2010) Immunity, inflammation, and cancer. Cell 140:883-
583 899.
584 Huang X, Li X, Ma Q, Xu Q, Duan W, Lei J, Zhang L, Wu Z (2015) Chronic alcohol exposure
585 exacerbates inflammation and triggers pancreatic acinar-to-ductal metaplasia through
586 PI3K/Akt/IKK. International journal of molecular medicine 35:653-663.

587 Koob GF (2014) Neurocircuitry of alcohol addiction: synthesis from animal models. Handbook of
588 clinical neurology 125:33-54.
589 Koob GF, Le Moal M (2008) Neurobiological mechanisms for opponent motivational processes
590 in addiction.
591 Koob GF, Volkow ND (2010) Neurocircuitry of Addiction. Neuropsychopharmacology : official
592 publication of the American College of Neuropsychopharmacology 35:217-238.
593 Lacagnina MJ, Rivera PD, Bilbo SD (2016) Glial and Neuroimmune Mechanisms as Critical
594 Modulators of Drug use and Abuse. Neuropsychopharmacology : official publication of the
595 American College of Neuropsychopharmacology.
596 Lam MP, Marinelli PW, Bai L, Gianoulakis C (2008) Effects of acute ethanol on opioid peptide
597 release in the central amygdala: an in vivo microdialysis study. Psychopharmacology
598 201:261-271.
599 Lappas M, Yee K, Permezel M, Rice GE (2005) Sulfasalazine and BAY 11-7082 Interfere with
600 the Nuclear Factor-κB and IκB Kinase Pathway to Regulate the Release of Proinflammatory
601 Cytokines from Human Adipose Tissue and Skeletal Muscle in Vitro. Endocrinology
602 146:1491-1497.
603 Liu J, Lewohl JM, Harris RA, Iyer VR, Dodd PR, Randall PK, Mayfield RD (2006) Patterns of
604 gene expression in the frontal cortex discriminate alcoholic from nonalcoholic individuals.
605 Neuropsychopharmacology : official publication of the American College of
606 Neuropsychopharmacology 31:1574-1582.
607 Liu X, Ding X, Deshmukh G, Liederer BM, Hop CE (2012) Use of the cassette-dosing approach
608 to assess brain penetration in drug discovery. Drug metabolism and disposition: the
609 biological fate of chemicals 40:963-969.
610 Maqbool A, Lattke M, Wirth T, Baumann B (2013) Sustained, neuron-specific IKK/NF-kappaB
611 activation generates a selective neuroinflammatory response promoting local
612 neurodegeneration with aging. Molecular neurodegeneration 8:40.

613 Mayfield J, Arends MA, Harris RA, Blednov YA (2016) Genes and Alcohol Consumption:
614 Studies with Mutant Mice. International review of neurobiology 126:293-355.
615 Moller C, Wiklund L, Sommer W, Thorsell A, Heilig M (1997) Decreased experimental anxiety
616 and voluntary ethanol consumption in rats following central but not basolateral amygdala
617 lesions. Brain Res 760:94-101.
618 Mulligan M, Ponomarev I, Hitzemann R, Belknap J, Tabakoff B, Harris R, Crabbe J (2006)
619 Toward Understanding the Genetics of Alcohol Drinking Through Transcriptome Meta-
620 Analysis. Proc Natl Acad Sci USA 103:6368 - 6373.
621 Nunez YO, Truitt JM, Gorini G, Ponomareva ON, Blednov YA, Harris RA, Mayfield RD (2013)
622 Positively correlated miRNA-mRNA regulatory networks in mouse frontal cortex during early
623 stages of alcohol dependence. BMC Genomics 14:725.
624 Ökvist A, Johansson S, Kuzmin A, Bazov I, Merino-Martinez R, Ponomarev I, Mayfield RD,
625 Harris RA, Sheedy D, Garrick T, Harper C, Hurd YL, Terenius L, Ekström TJ, Bakalkin G,
626 Yakovleva T (2007) Neuroadaptations in Human Chronic Alcoholics: Dysregulation of the
627 NF-κB System. PLoS ONE 2:e930.
628 Osterndorff-Kahanek E, Ponomarev I, Blednov YA, Harris RA (2013) Gene expression in brain
629 and liver produced by three different regimens of alcohol consumption in mice: comparison
630 with immune activation. PLoS One 8:e59870.
631 Osterndorff-Kahanek EA, Becker HC, Lopez MF, Farris SP, Tiwari GR, Nunez YO, Harris RA,
632 Mayfield RD (2015) Chronic ethanol exposure produces time- and brain region-dependent
633 changes in gene coexpression networks. PLoS One 10:e0121522.
634 Pastor IJ, Laso FJ, Romero A, Gonzalez-Sarmiento R (2005) Interleukin-1 gene cluster
635 polymorphisms and alcoholism in Spanish men. Alcohol and alcoholism (Oxford,
636 Oxfordshire) 40:181-186.

637 Pastor IJ, Laso FJ, Àvila JJ, Rodriguez RE, González-Sarrniento R (2000) Polymorphism in the
638 Interleukin-1 Receptor Antagonist Gene Is Associated With Alcoholism in Spanish Men.
639 Alcoholism: Clinical and Experimental Research 24:1479-1482.
640 Perkins ND (2007) Integrating cell-signalling pathways with NF-kappaB and IKK function. Nat
641 Rev Mol Cell Biol 8:49-62.
642 Podolin PL, Callahan JF, Bolognese BJ, Li YH, Carlson K, Davis TG, Mellor GW, Evans C,
643 Roshak AK (2005) Attenuation of murine collagen-induced arthritis by a novel, potent,
644 selective small molecule inhibitor of IkappaB Kinase 2, TPCA-1 (2-[(aminocarbonyl)amino]-
645 5-(4-fluorophenyl)-3-thiophenecarboxamide), occurs via reduction of proinflammatory
646 cytokines and antigen-induced T cell Proliferation. J Pharmacol Exp Ther 312:373-381.
647 Roberto M, Madamba SG, Stouffer DG, Parsons LH, Siggins GR (2004a) Increased GABA
648 release in the central amygdala of ethanol-dependent rats. J Neurosci 24:10159-10166.
649 Roberto M, Bajo M, Crawford E, Madamba SG, Siggins GR (2006) Chronic ethanol exposure
650 and protracted abstinence alter NMDA receptors in central amygdala.
651 Neuropsychopharmacology : official publication of the American College of
652 Neuropsychopharmacology 31:988-996.
653 Roberto M, Schweitzer P, Madamba SG, Stouffer DG, Parsons LH, Siggins GR (2004b) Acute
654 and chronic ethanol alter glutamatergic transmission in rat central amygdala: an in vitro and
655 in vivo analysis. J Neurosci 24:1594-1603.
656 Robinson G, Most D, Ferguson LB, Mayfield J, Harris RA, Blednov YA (2014) Neuroimmune
657 pathways in alcohol consumption: evidence from behavioral and genetic studies in rodents
658 and humans. International review of neurobiology 118:13-39.
659 Russo SJ et al. (2009) Nuclear factor kappa B signaling regulates neuronal morphology and
660 cocaine reward. J Neurosci 29:3529-3537.
661 Saiz PA, Garcia-Portilla MP, Florez G, Corcoran P, Arango C, Morales B, Leza JC, Alvarez S,
662 Diaz EM, Alvarez V, Coto E, Nogueiras L, Bobes J (2009) Polymorphisms of the IL-1 gene

663 complex are associated with alcohol dependence in Spanish Caucasians: data from an
664 association study. Alcoholism, clinical and experimental research 33:2147-2153.
665 Scheidereit C (2006) IkappaB kinase complexes: gateways to NF-kappaB activation and
666 transcription. Oncogene 25:6685-6705.
667 Schmid JA, Birbach A (2008) IkappaB kinase beta (IKKbeta/IKK2/IKBKB)--a key molecule in
668 signaling to the transcription factor NF-kappaB. Cytokine & growth factor reviews 19:157-
669 165.
670 Schmittgen TD, Livak KJ (2008) Analyzing real-time PCR data by the comparative CT method.
671 Nat Protocols 3:1101-1108.
672 Sunami Y, Leithauser F, Gul S, Fiedler K, Guldiken N, Espenlaub S, Holzmann KH, Hipp N,
673 Sindrilaru A, Luedde T, Baumann B, Wissel S, Kreppel F, Schneider M, Scharffetter-
674 Kochanek K, Kochanek S, Strnad P, Wirth T (2012) Hepatic activation of IKK/NFkappaB
675 signaling induces liver fibrosis via macrophage-mediated chronic inflammation. Hepatology
676 (Baltimore, Md) 56:1117-1128.
677 Szabo G, Lippai D (2014) Converging actions of alcohol on liver and brain immune signaling.
678 International review of neurobiology 118:359-380.
679 Tanaka M, Fuentes ME, Yamaguchi K, Durnin MH, Dalrymple SA, Hardy KL, Goeddel DV
680 (1999) Embryonic lethality, liver degeneration, and impaired NF-kappa B activation in IKK-
681 beta-deficient mice. Immunity 10:421-429.
682 Thiele TE, Navarro M (2014) "Drinking in the dark" (DID) procedures: a model of binge-like
683 ethanol drinking in non-dependent mice. Alcohol (Fayetteville, NY) 48:235-241.
684 Warden A, Erickson E, Robinson G, Harris RA, Mayfield RD (2016) The neuroimmune
685 transcriptome and alcohol dependence: Potential for targeted therapies. Pharmacogenetics
686 in press.
687 Zhang X, Zhang G, Zhang H, Karin M, Bai H, Cai D (2008) Hypothalamic IKKβ/NF-κB and ER
688 Stress Link Overnutrition to Energy Imbalance and Obesity. Cell 135:61-73.

689

690 **Table Legend**

691 **Table 1. Ethanol-induced changes in NFKB/REL gene targets in mouse.** Ethanol
692 administration produced numerous changes in NFKB/REL gene targets in mouse central
693 amygdala (CeA), nucleus accumbens (NAc) and prefrontal cortex (PFC). Ingenuity Pathway
694 Analysis was used to curate gene targets. Gene target identification included both human and
695 mouse databases. Human nomenclature is used here. Adjusted p values are listed using an
696 FDR of $p<0.001$. Experimental details are provided in Osterndorff-Kahanek et al., 2015.

697 **Figure Legends**

698 **Figure 1.** Effect of systemic administration of IKKβ inhibitors on ethanol (EtOH) intake and
699 preference after the first 6 h of a continuous 24-h two-bottle choice test in C57BL/6J mice. A-C.
700 TPCA-1 (30 and 50 mg) vs. saline treated (n=13 per group). D-F. Sulfasalazine (50 and 100
701 mg) vs. saline treated (n=6 per group). A and D. 15% ethanol consumption (g/kg/6h). B and E.
702 Preference for ethanol. C and F. Total fluid intake (g/kg/6h). Day 2 in each panel shows the
703 averages of 2 days of saline injections for each group ± SEM. Remaining time points are the
704 averages of 2 days of drinking ± SEM. Significant main effect of drug treatment is shown by the
705 p-value beneath the treatment dose (two-way ANOVA with repeated measures). Significant
706 effect of each drug compared with the corresponding saline group is indicated by the symbols
707 above each time point (Bonferroni post-hoc test for multiple comparisons *$p<0.05$, **$p<0.01$,
708 ***$p<0.001$ or Student's t-test $^{\#}p<0.05$).

709 **Figure 2.** Effect of IKKβ inhibitors on ethanol (EtOH) intake and preference after the first 3 h in a
710 limited access two-bottle choice drinking-in-the-dark test in C57BL/6J mice. A-C. 50 mg/kg
711 TPCA-1 vs. saline treated (n=6 per group). D-F. 100 mg/kg sulfasalazine-treated (n=8 per
712 group). A and D. 15% ethanol consumption (g/kg/3h). B and E. Preference for ethanol. C and F.
713 Total fluid intake (g/kg/3h). Day 2 in each panel shows the averages of 2 days of saline

714 injections for each group ± SEM. Remaining time points are the averages of 2 days of drinking ±
715 SEM. Significant main effect of drug treatment is shown by the p-value (two-way ANOVA with
716 repeated measures). Significant effect of each drug compared with the corresponding saline
717 group is indicated by the symbols above each time point (Bonferroni post-hoc test for multiple
718 comparisons *p<0.05, **p<0.01, ***p<0.001).

719 **Figure 3.** IKKβ protein knockdown (3 and 8 weeks post injection) in NAc of *Ikkβ*$^{F/F}$ mice. A
720 fluorescent light microscope image of a representative stain from the 3-week post-injection time
721 point in NAc is shown. A. anti-IKKβ fluorescently-labeled antibody. B. anti-EGFP fluorescently-
722 labeled antibody. C. Overlay of A and B ("IKKβ –" represents transduced cells without IKKβ and
723 "IKKβ +" represents transduced cells with IKKβ) D. Knockdown of IKKβ (LV-EGFP-Cre)
724 measured by IKKβ-positive cells colocalized with EGFP-positive cells relative to their time
725 matched control (LV-EGFP-Empty). The mean ± SEM of 8 fields of view (20x) per mouse for 4
726 mice are shown (n=4 for each group: 3 weeks after LV-EGFP-Cre, 3 weeks after LV-EGFP-
727 Empty, 8 weeks after LV-EGFP-Cre, 8 weeks after LV-EGFP-Empty). (Student's t-test **p<0.01,
728 ***p<0.001).

729 **Figure 4.** Effect of IKKβ knockdown in NAc on ethanol (EtOH) intake and preference during the
730 24-h two-bottle choice test in *Ikkβ*$^{F/F}$ mice. A-C. n=32 animals injected with LV-Cre-EGFP and
731 n=20 injected with LV-Cre-Empty. A. Ethanol consumption (g/kg/24 h). B. Preference for
732 ethanol. C. Total fluid intake (g/kg/24 h). Each point is the average of 2 days of drinking ± SEM.
733 Significant main effect of treatment is shown by the p-value (two-way ANOVA with repeated
734 measures). Significant effect of LV-EGFP-Cre compared with LV-EGFP-Empty treatment is
735 indicated by symbols above each time point (Bonferroni post-hoc test for multiple comparisons
736 *p<0.05, **p<0.01). n=32 animals injected with LV-Cre-EGFP and n=20 injected with LV-Cre-
737 Empty.

738 **Figure 5.** Effect of IKKβ knockdown in CeA on ethanol (EtOH) intake and preference during a
739 continuous 24-h two-bottle choice test in *Ikkβ*$^{F/F}$ mice. A. Ethanol consumption (g/kg/24 h). B.

Preference for ethanol. C. Total fluid intake (g/kg/24 h). Significant main effect of treatment is shown by the p-value (two-way ANOVA with repeated measures). Significant post-hoc effect of LV-EGFP-Cre compared with LV-EGFP-Empty treatment is indicated by *p<0.05 (Bonferroni test for multiple comparisons). n=20 injected with LV-EGFP-Cre and n=10 injected with LV-EGFP-Empty.

Figure 6. Lentiviral-mediated knockdown of IKKβ in the NAc and CeA had no effect on saccharin preference or total fluid intake using a continuous 24-h two-bottle choice test in *Ikkβ*$^{F/F}$ mice. The effect of IKKβ knockdown in NAc (n=32 LV-EGFP-Cre, n=20 LV-EGFP-Empty) is shown in panels A (Preference for saccharin) and B (Total fluid intake (g/kg/24 h). The effect of IKKβ knockdown in CeA (n=20 LV-EGFP-Cre, n=10 LV-EGFP-Empty) is shown in panels C (Preference for saccharin) and D (Total fluid intake (g/kg/24 h). Each point is the average of 2 days of drinking ± SEM.

Figure 7. Injection target verification of lentiviral-mediated IKKβ knockdown in the NAc and CeA. Composite microscope images of a coronal section in the (A) NAc or (C) CeA of a representative lentiviral injection using fluorescent microscopy (on left) to show EGFP marker signal (green), and bright-field (on right) to demonstrate neuroanatomy. Coronal brain atlas figures of the injection sites with blue circles indicating the (B) NAc or (D) CeA, and the green ovals illustrating the typical lentiviral injection location and spread.

Figure 8. IKKβ protein levels and mRNA expression of IKKβ, TNF-α, and IL-6 at the injection site upon completion of behavioral studies. IKKβ protein levels in NAc and CeA (A) (n=5 per group: NAc LV-EGFP-Cre, NAc LV-EGFP-Empty, CeA LV-EGFP-Cre, and CeA LV-EGFP-Empty). mRNA levels of IKKβ (B), TNF-α (C), and IL-6 (D) in the NAc (n=10 LV-EGFP-Cre, n=5 LV-EGFP-Empty) and CeA (n=5 LV-EGFP-Cre, n=5 LV-EGFP-Empty). Values are shown relative to LV-EGFP-Empty treated mice. IKKβ protein levels were analyzed using immunohistochemistry. IKKβ mRNA levels at the target site in the NAc and CeA were assessed

765 by quantitative RT-PCR and normalized relative to GADPH. **p<0.01, ***p<0.001 determined by
766 Student t test. All data are shown as the mean ± SEM.
767 **Figure 9.** Cell type-specific localization of IKKβ in the NAc and CeA. Representative fluorescent
768 light microscope images illustrating cell-type specific antibodies in the first columns (A. anti-
769 NeuN for neurons; D. anti-GFAP for astrocytes; G. anti-Iba1 for microglia), anti-IKKβ stains in
770 the second columns (B, E, H), and overlay of the first two in the third columns (C, F, I). Arrows
771 illustrate cells showing colocalization of anti-IKKβ and cell type-specific stains.
772 **Figure 10.** Cell-type trophism of lentiviral vectors in the NAc and CeA. Representative
773 fluorescent light microscope images illustrating cell-type specific stains in the first columns (A.
774 anti-GFAP for astrocytes; D. anti-NeuN for neurons; G. anti-Iba1 for microglia), anti-GFP stains
775 in the second columns (B, E, H), and overlay of the first two in the third columns (C, F, I).
776 Arrows illustrate cells showing co-expression of anti-GFP and cell type-specific stains.
777

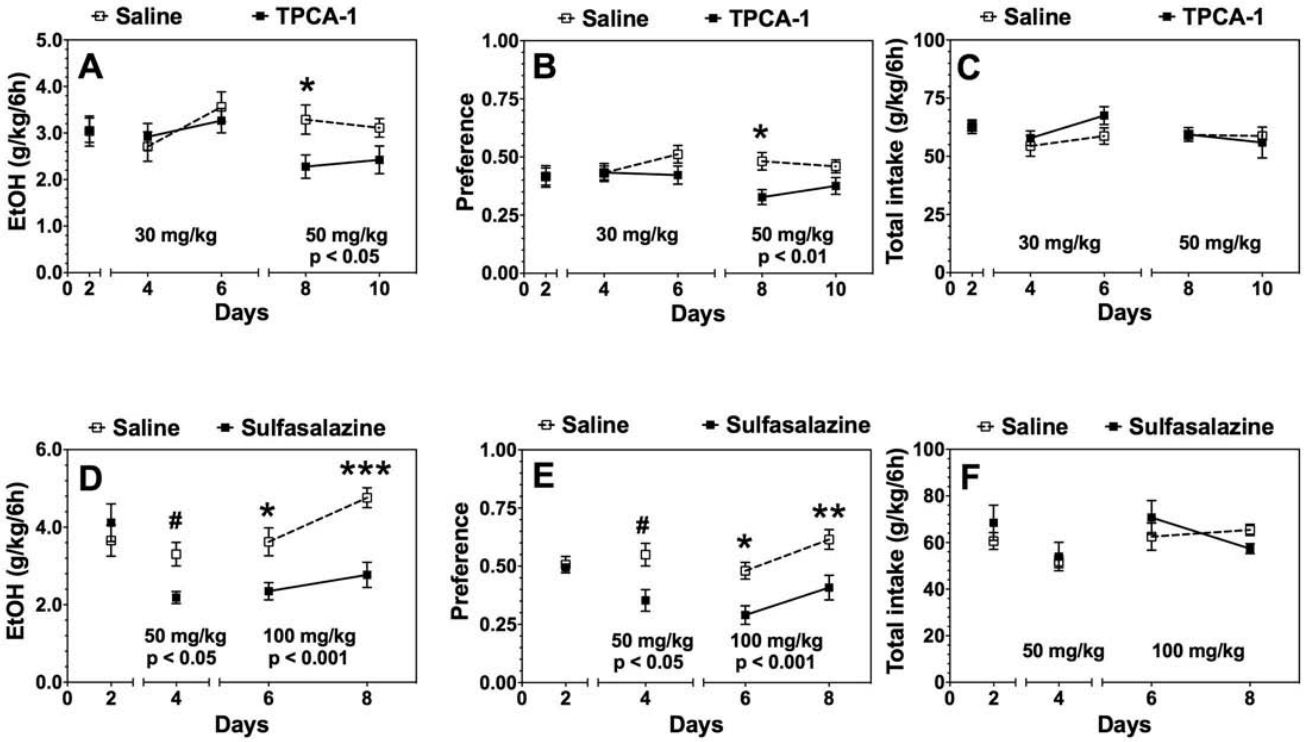

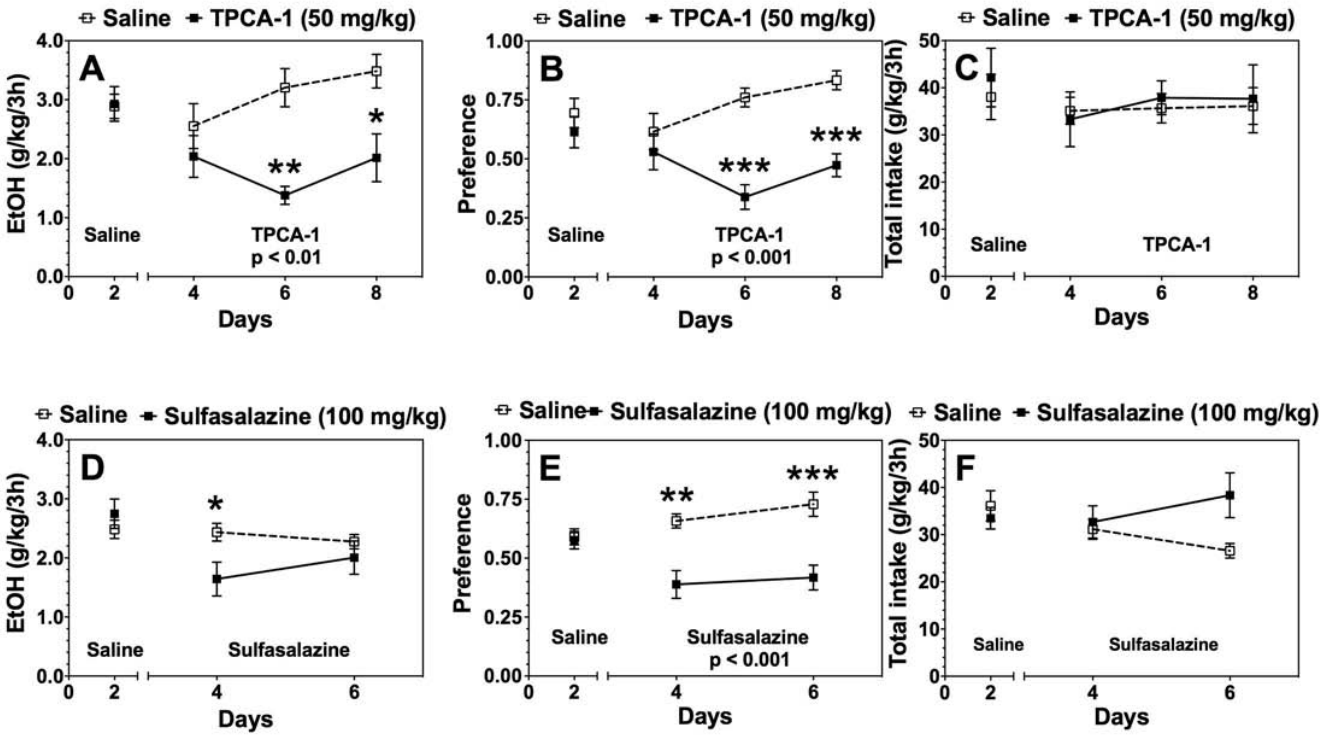

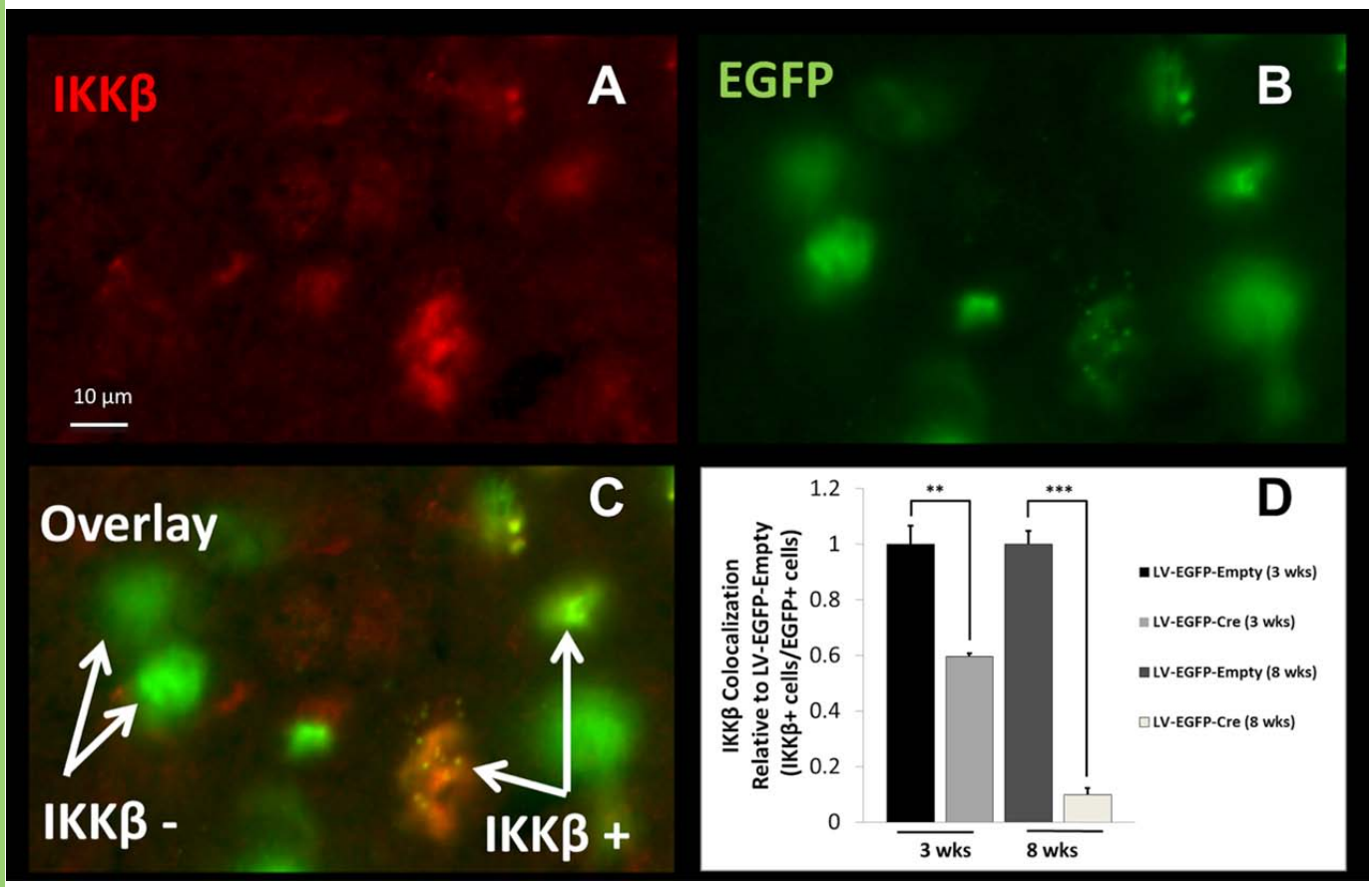

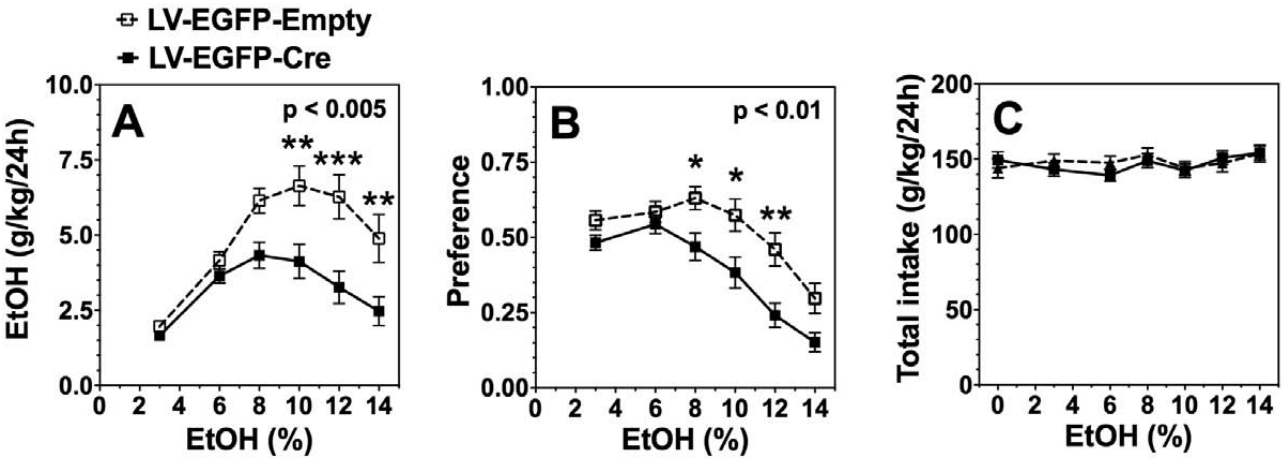

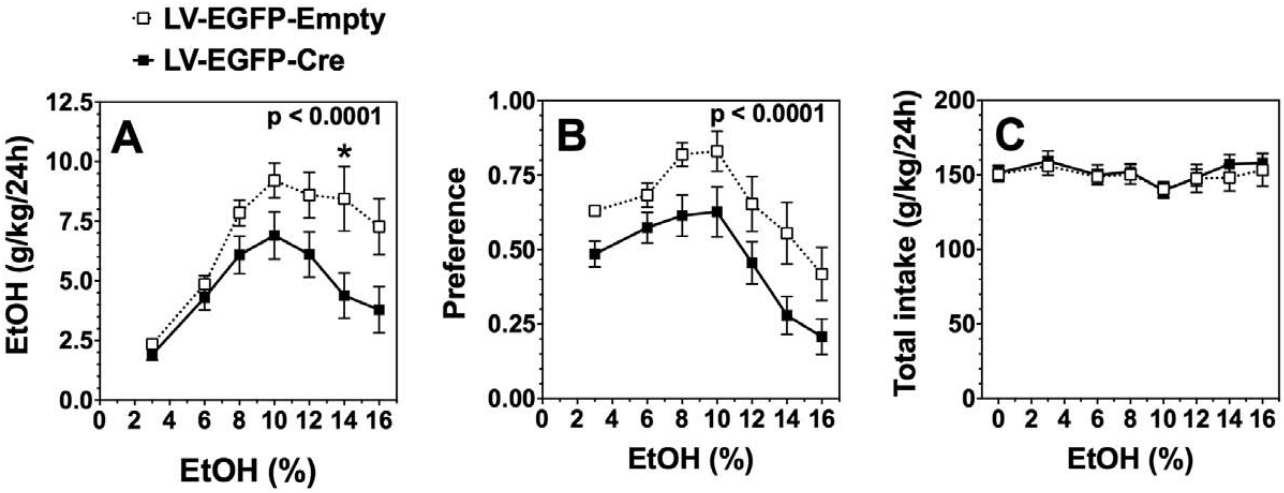

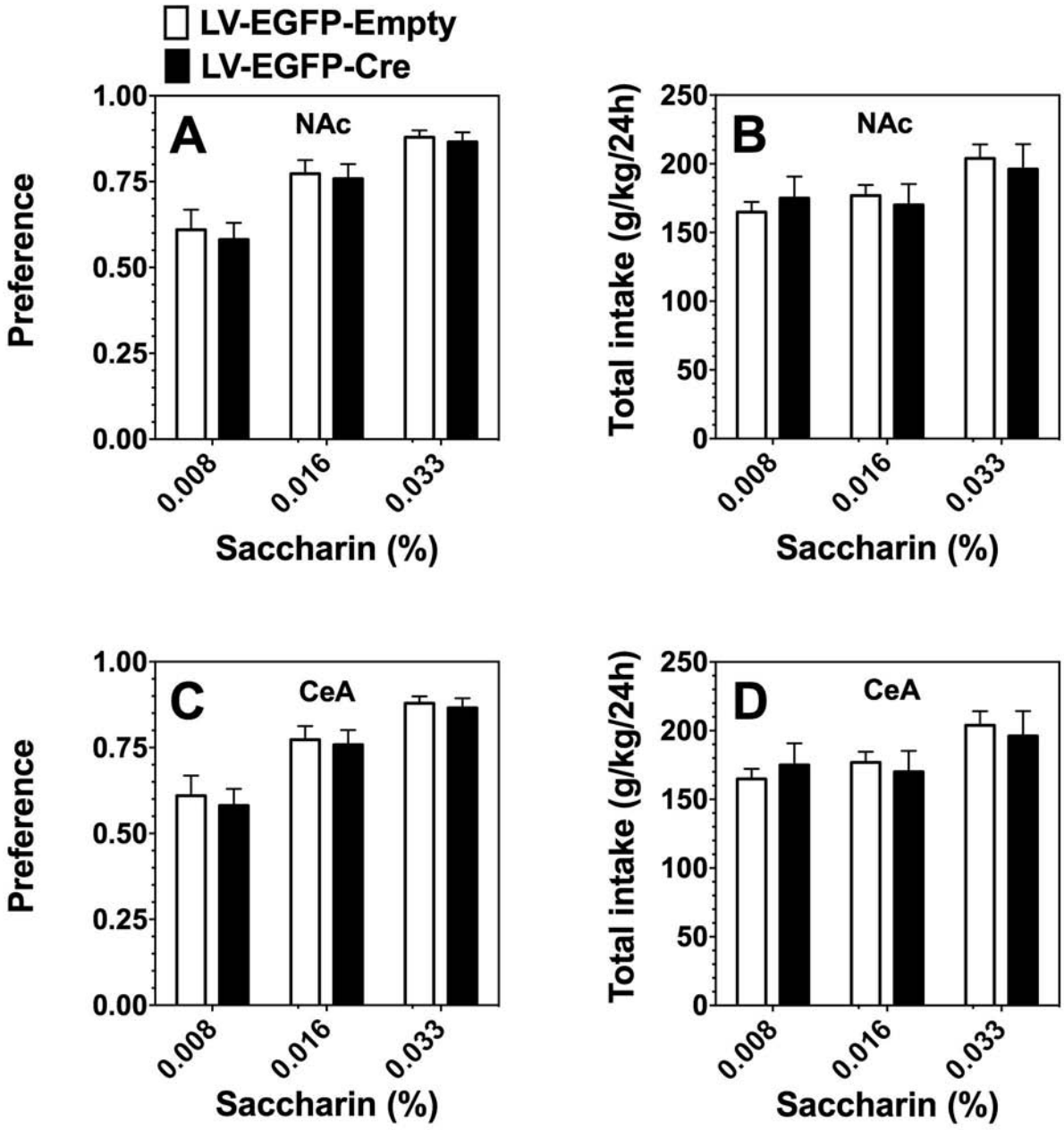

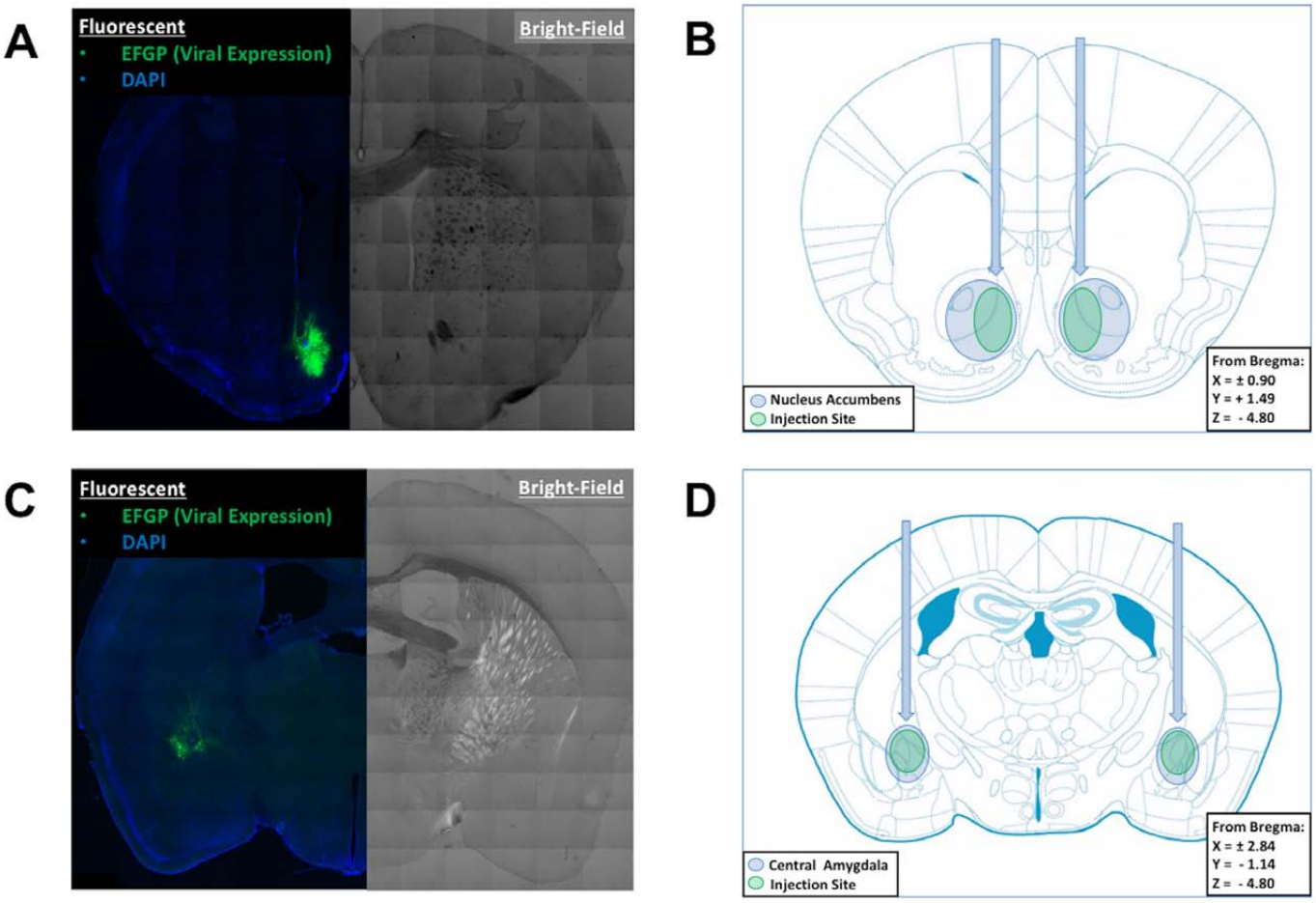

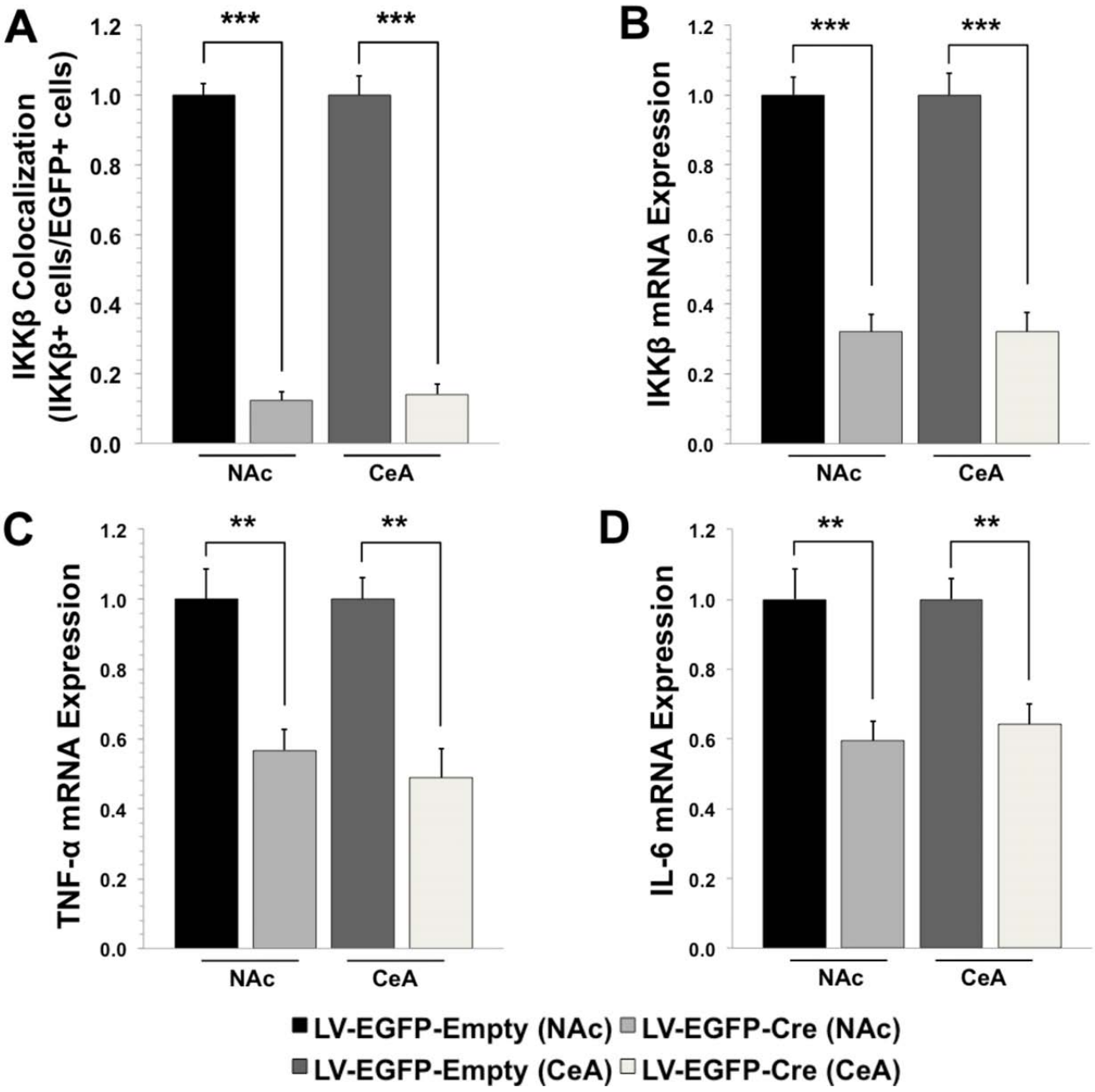

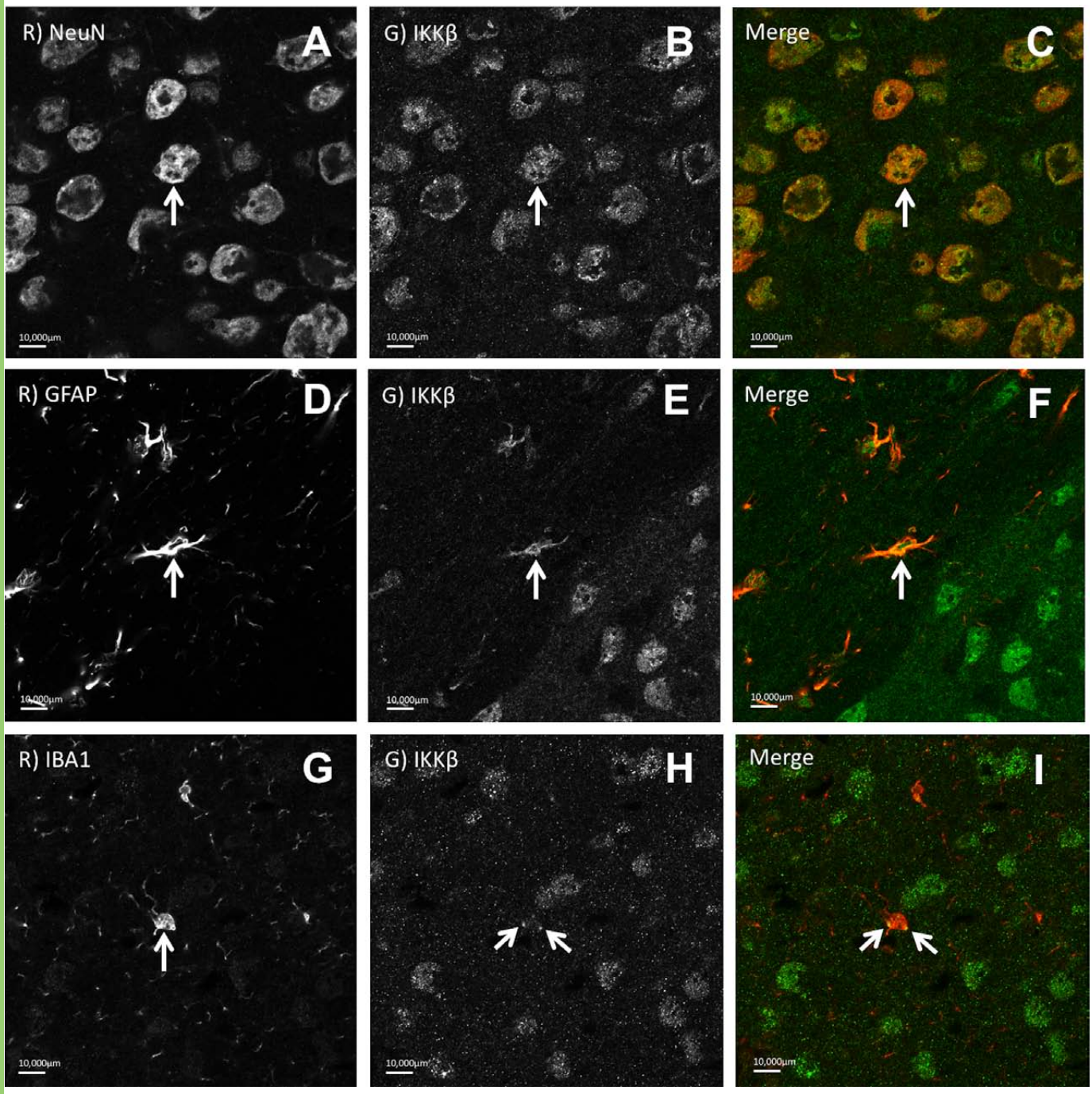

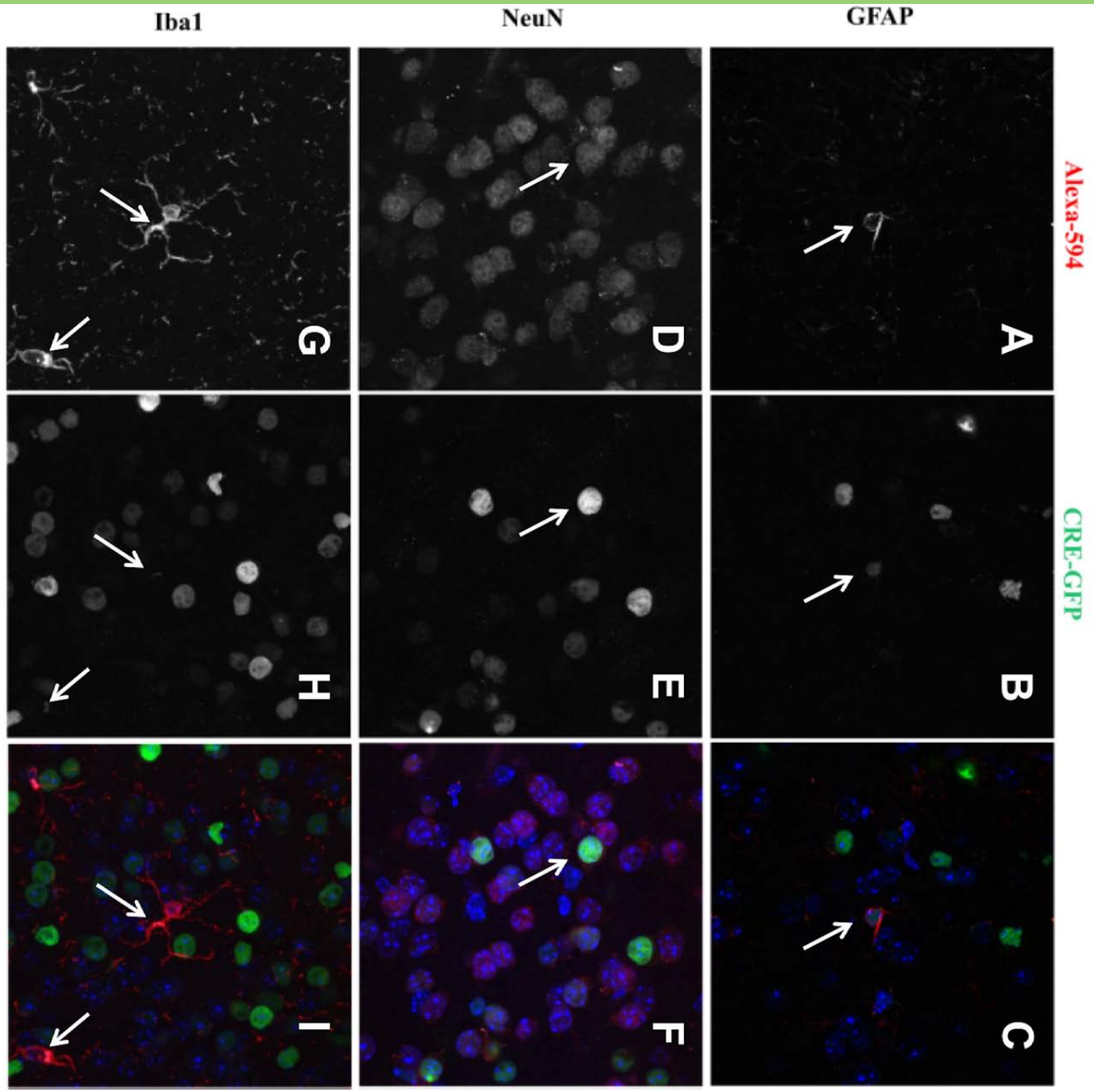

Table 1. Ethanol-induced changes in NFKB/REL gene targets in mouse.

CeA		NAc		PFC	
Illumina Probe ID	**NFKB-REL Targets (IPA)**	**Illumina Probe ID**	**NFKB- REL Targets (IPA)**	**Illumina Probe ID**	**NFKB- REL Targets (IPA)**
ILMN_2738825	*ACTA1*	ILMN_2878060	*ANXA6*	ILMN_2878060	*ANXA6*
ILMN_2739999	*B2M*	ILMN_2739999	*B2M*	ILMN_1221503	*CCND1*
ILMN_1216746	*B2M*	ILMN_1216746	*B2M*	ILMN_2601471	*CCND1*
ILMN_2717613	*CDK2*	ILMN_2706514	*BCL2*	ILMN_2931411	*CCT3*
ILMN_2756435	*CEBPB*	ILMN_2716567	*BNIP3L*	ILMN_2846775	*CDKN1A*
ILMN_2609813	*CHI3L1*	ILMN_2756435	*CEBPB*	ILMN_2634083	*CDKN1A*
ILMN_1224754	*CKB*	ILMN_2959480	*EIF4A1*	ILMN_2846776	*CDKN1A*
ILMN_2747651	*HAT1*	ILMN_2718815	*FAF1*	ILMN_2992403	*CINP*
ILMN_2624153	*HES5*	ILMN_2994806	*H2AFJ*	ILMN_2627041	*CX3CL1*
ILMN_1253414	*HES5*	ILMN_2648292	*H3F3A/H3F3B*	ILMN_1256348	*DNTTIP1*
ILMN_2791952	*HES6*	ILMN_1253414	*HES5*	ILMN_2737713	*EDN1*
ILMN_1222313	*HIST1H4J*	ILMN_2791952	*HES6*	ILMN_2903945	*GADD45G*
ILMN_2924419	*HLA-A*	ILMN_2855315	*HIST1H1C*	ILMN_2791952	*HES6*
ILMN_2835683	*HLA-A*	ILMN_2924419	*HLA-A*	ILMN_2835683	*HLA-A*
ILMN_1235470	*HNRNPC*	ILMN_2835683	*HLA-A*	ILMN_3156604	*HMGB2*
ILMN_1239021	*HNRNPM*	ILMN_2715802	*HMGA1*	ILMN_2664319	*IRF3*
ILMN_2646625	*JUN*	ILMN_1235470	*HNRNPC*	ILMN_2646625	*JUN*
ILMN_2878071	*LYZ*	ILMN_2511051	*HNRNPC*	ILMN_3001914	*NFKBIA*
ILMN_2640883	*NDE1*	ILMN_2921103	*HNRNPM*	ILMN_2596979	*NRARP*
ILMN_2596979	*NRARP*	ILMN_2921095	*HNRNPM*	ILMN_3158919	*PRKCZ*
ILMN_1242466	*PSMB9*	ILMN_1239021	*HNRNPM*	ILMN_2647533	*SLC41A3*
ILMN_2717621	*RPS15A*	ILMN_2646625	*JUN*	ILMN_2938893	*SMAD3*
ILMN_2883164	*SERPINE2*	ILMN_1258376	*KCNK6*	ILMN_2701664	*TSC22D3*
ILMN_2701664	*TSC22D3*	ILMN_1258526	*LGALS3BP*	ILMN_3150811	*TSC22D3*
ILMN_3150811	*TSC22D3*	ILMN_2878071	*LYZ*	ILMN_3112873	*TXNIP*
ILMN_3121255	*VEGFA*	ILMN_2640883	*NDE1*		
		ILMN_2596979	*NRARP*		
		ILMN_2790181	*PHGDH*		
		ILMN_1234766	*PPME1*		
		ILMN_2833378	*PRKACA*		
		ILMN_1242466	*PSMB9*		
		ILMN_1248316	*PTGDS*		
		ILMN_2728729	*SDC4*		
		ILMN_3027751	SORBS1		

		ILMN_2988299	SRF		
		ILMN_2692615	TGM2		
		ILMN_2701664	TSC22D3		
		ILMN_3150811	TSC22D3		
		ILMN_3112873	TXNIP		

Ethanol administration produced numerous changes in NFKB/REL gene targets in mouse central amygdala (CeA), nucleus accumbens (NAc) and prefrontal cortex (PFC). Ingenuity Pathway Analysis was used to curate gene targets. Gene target identification included both human and mouse databases. Human nomenclature is used here. Adjusted p values are listed using an FDR of $p<0.001$. Experimental details are provided in Osterndorff-Kahanek et al., 2015.